Supplemental Tables and Figures
Chapter II

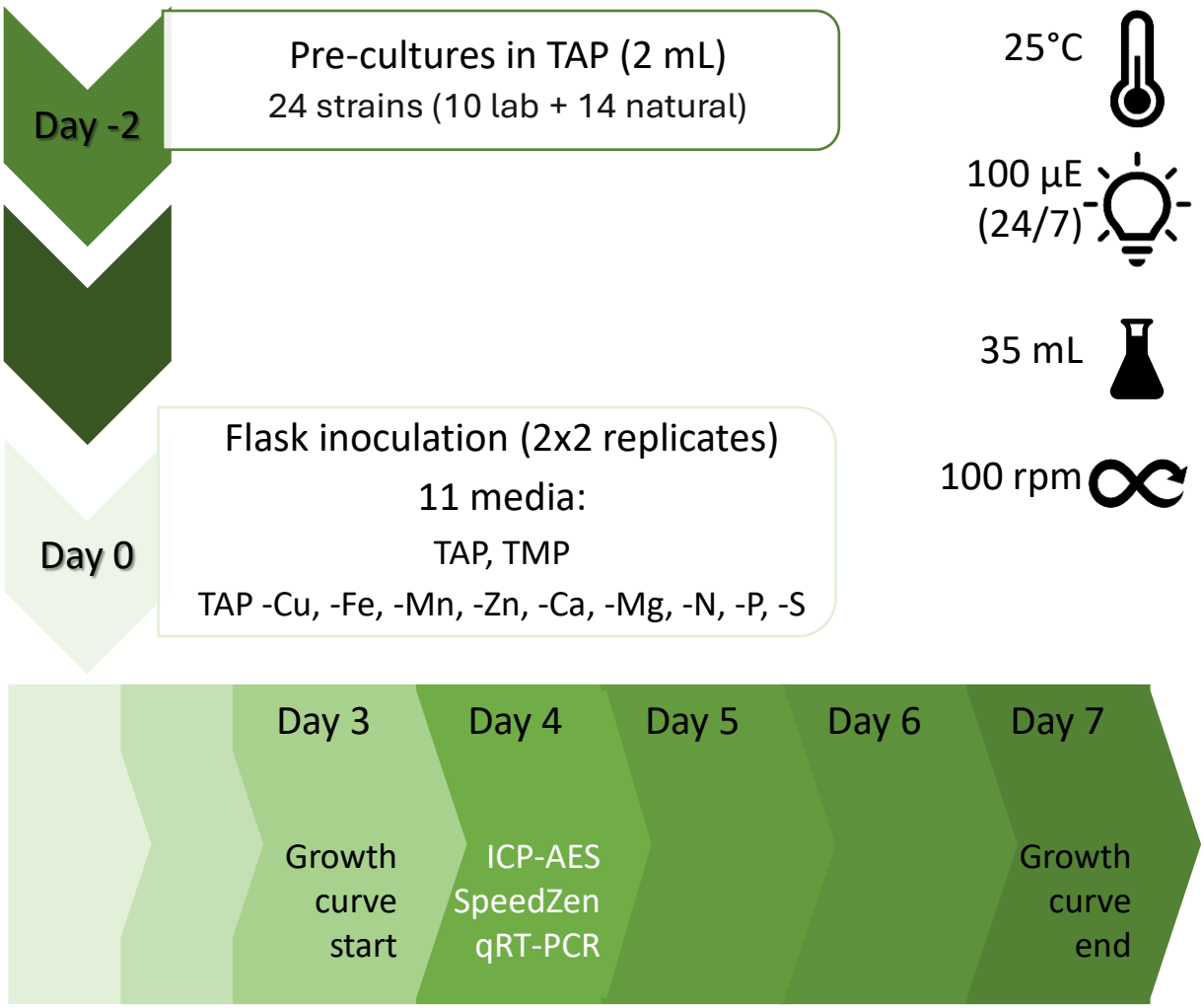

Figure S.II.1. Schematic representation of the experimental design. Two days before the experiment, precultures of the 24 strains were initiated. On the day of the experiment, the precultures were used to inoculate 2 replicates in flasks containing treatment media. Cell density ($OD7_{50nm}$) was measured once a day from day 3 to day 7, and at day 4 a sample was collected for ionome (ICP-AES), photosynthesis (SpeedZen) and marker gene expression (qRT-PCR) analyses. The experiment was performed twice (n = 4) independently in 35 mL of media, at 25°C, 24h photoperiod (100 µmol m^{-2} s^{-1}) with agitation (100 rpm).

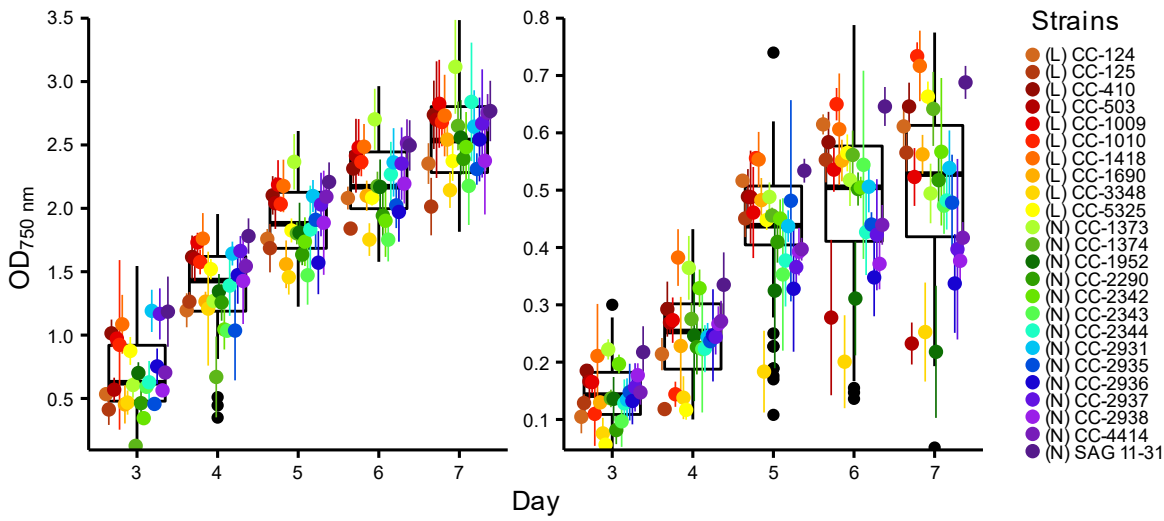

Figure S.II.2. Growth variation of 24 Chlamydomonas strains grown in TAP (A) and TMP (B). Growth was measured as optical density at 750 nm (OD_{750nm}) from day 3 to day 7. The boxes represent the 1st quantile, median and 3rd quartile of the data for all strains, and the whiskers extend from the median ± 1.5 interquartile range whereas outliers are represented by black dots. Each coloured dot represents the mean ± SD for each strain. Values are from 2 independent experiments, with 2 replicates each (n=4). The laboratory strains (L) are coloured in a yellow-dark red scale and the natural strains (N) are coloured in green-violet scale. The strains are ordered according to the colour key.

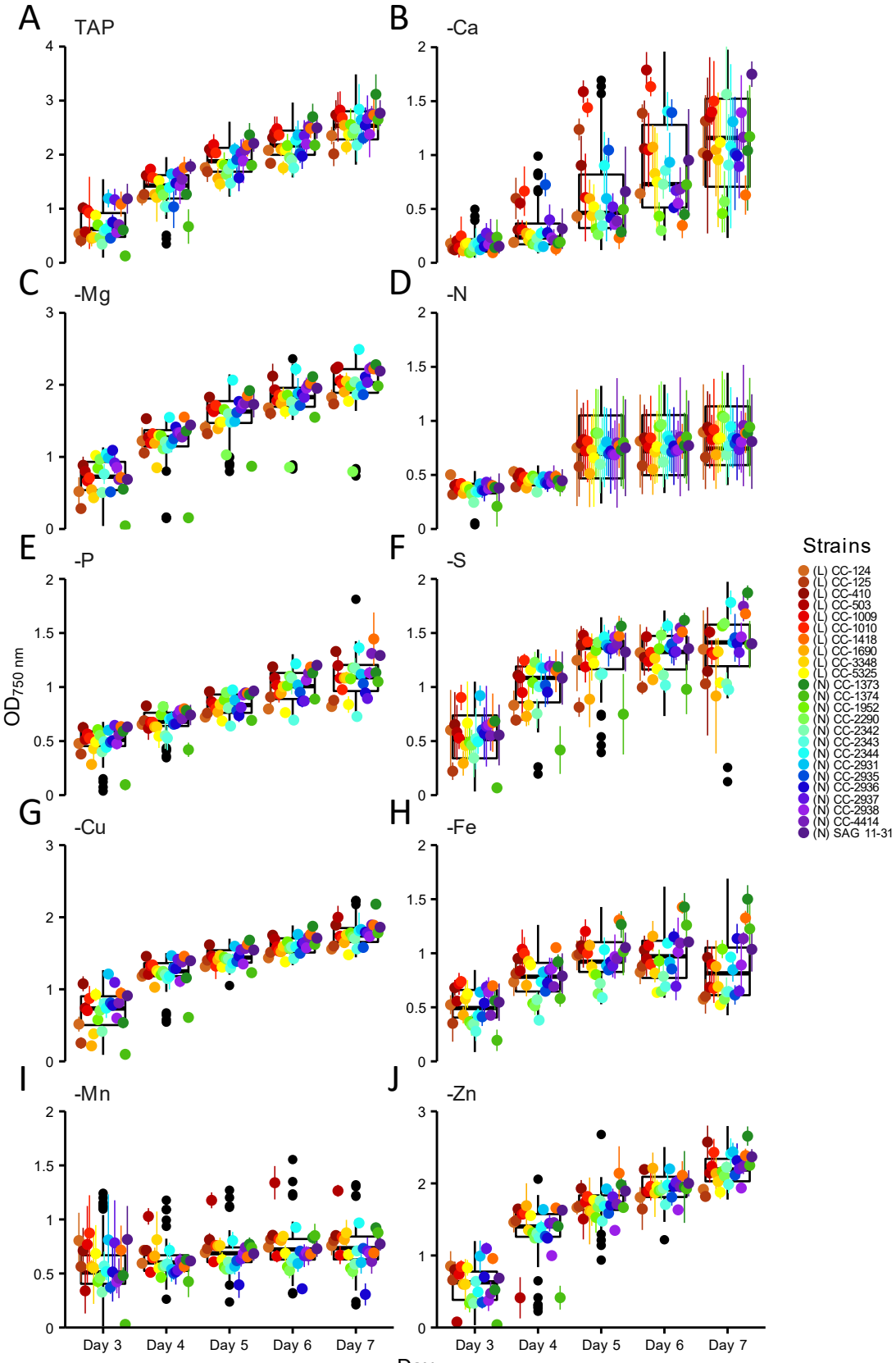

Figure S.II.3. Variation of the impact of mineral deficiencies on growth of 24 Chlamydomonas strains. Growth was measured as optical density at 750 nm (OD_{750nm}) from day 3 to day 7. The strains were cultured on TAP control medium **(A)** and on TAP with single deficiencies of 5 macroelements [-Ca **(B)**, -Mg **(C)**, -N **(D)**, -P **(E)**, -S **(F)**] and 4 microelements [-Cu **(G)**, -Fe **(H)**, -Mn **(I)**, -Zn **(J)**]. The boxes represent the 1st quartile, median and 3rd quartile of the raw data, and the whiskers extend from the median ± 1.5 interquartile range whereas outliers are represented by black dots. Each coloured dot represents the mean ± SD for each strain. Values are from 2 independent experiments, with 2 replicates each (n=4). The laboratory strains (L) are coloured in a yellow-dark red scale and the natural strains (N) are coloured in green-violet scale. The strains are ordered according to the colour key.

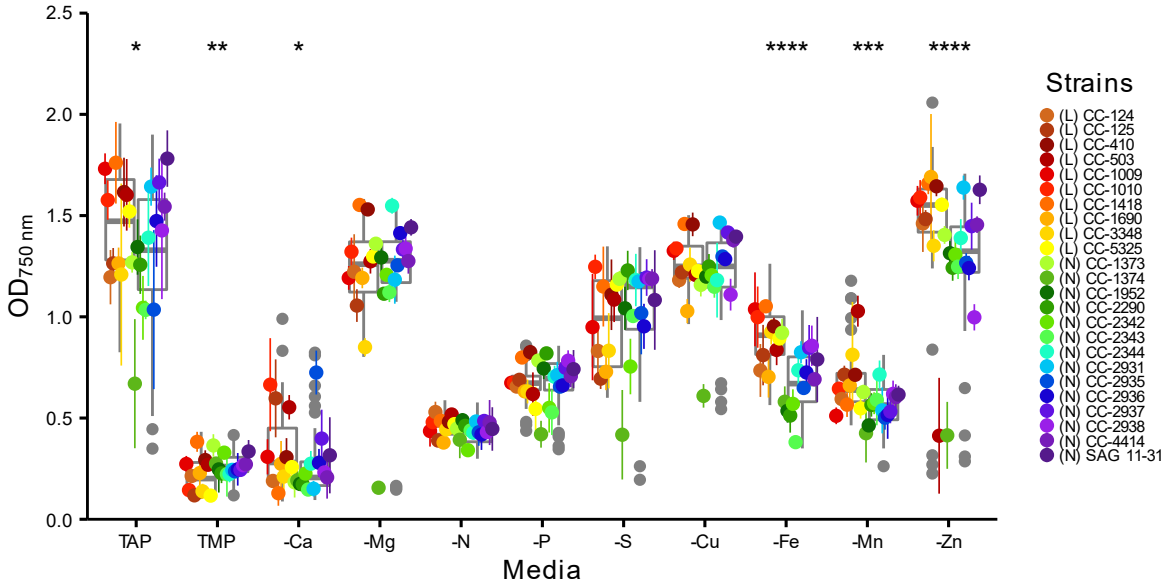

Figure S.II.4. Variation of the impact of nutrient deficiencies on growth of laboratory vs natural Chlamydomonas strains. Growth was measured as optical density at 750 nm (OD_{750nm}), at day 4 of culture on TAP (mixotrophy, control), TMP and TAP with single deficiencies for 5 macroelements (-Ca, -Mg, -N, -P, -S) or 4 microelements (-Cu, -Fe, -Mn, -Zn). Each coloured dot represents the mean ± SD for each strain. Values are from 2 independent experiments, with 2 replicates each (n=4). The laboratory strains (L) are coloured in a yellow-dark red scale and the natural strains (N) are coloured in green-violet. The strains are ordered according to the colour key. For each treatment, OD_{750nm} average values for N and L strains were compared using the Wilcoxon test, and significant differences are indicated with *: p <= 0.05, **: p <= 0.01, ***: p <= 0.001 and ****: p <= 0.0001. The boxes represent the 1st quartile, median and 3rd quartile of the raw data, and the whiskers extend from the median ± 1.5 interquartile range whereas outliers are represented by grey dots.

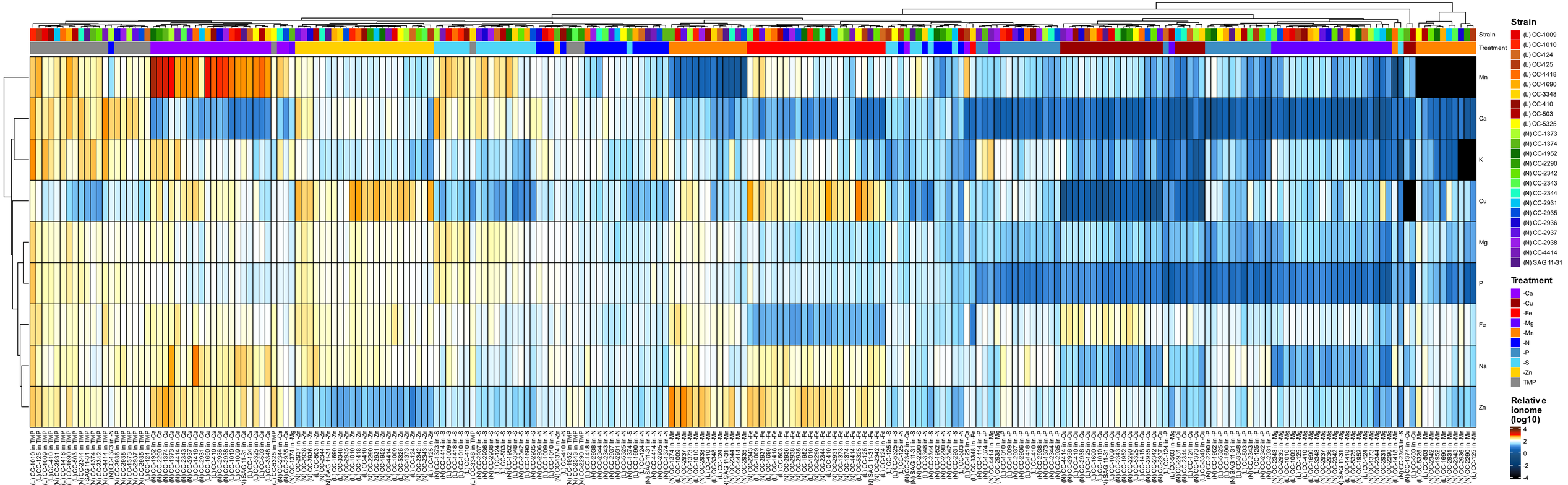

Figure S.II.5. Clustering of 24 Chlamydomonas strains exposed to the 9 nutrient deficiencies and autotrophy based on their ionome profiles. Samples were analysed by ICP-AES at day 4 of growth TMP (autotrophy) and on TAP with single deficiencies of 5 macroelements (-Ca, -Mg, -N, -P, -S) or 4 microelements (-Cu, -Fe, -Mn, -Zn). The concentrations of 9 elements (Ca, Cu, Fe, K, Mg, Mn, Na, P, Zn) are average concentrations relative to the TAP condition. For easier representation, null values were replaced by $10^{[-4]}$. The data was scaled using a log10 transformation and the control value, represented as 2 (100% = $10^{[2]}$ %), is coloured in white. Dendrograms represent the Euclidean distance clustered by complete linkage. Strain origin is shown between brackets as well as on the outermost right column where the natural strains (N) are coloured in a yellow-dark red scale and the laboratory strains (L) are coloured in green-violet scale. The treatment is colour-coded in the second to the right column, with autotrophy in grey, macronutrient deficiency in violet- blue scale and micronutrient deficiency in red-yellow scale.

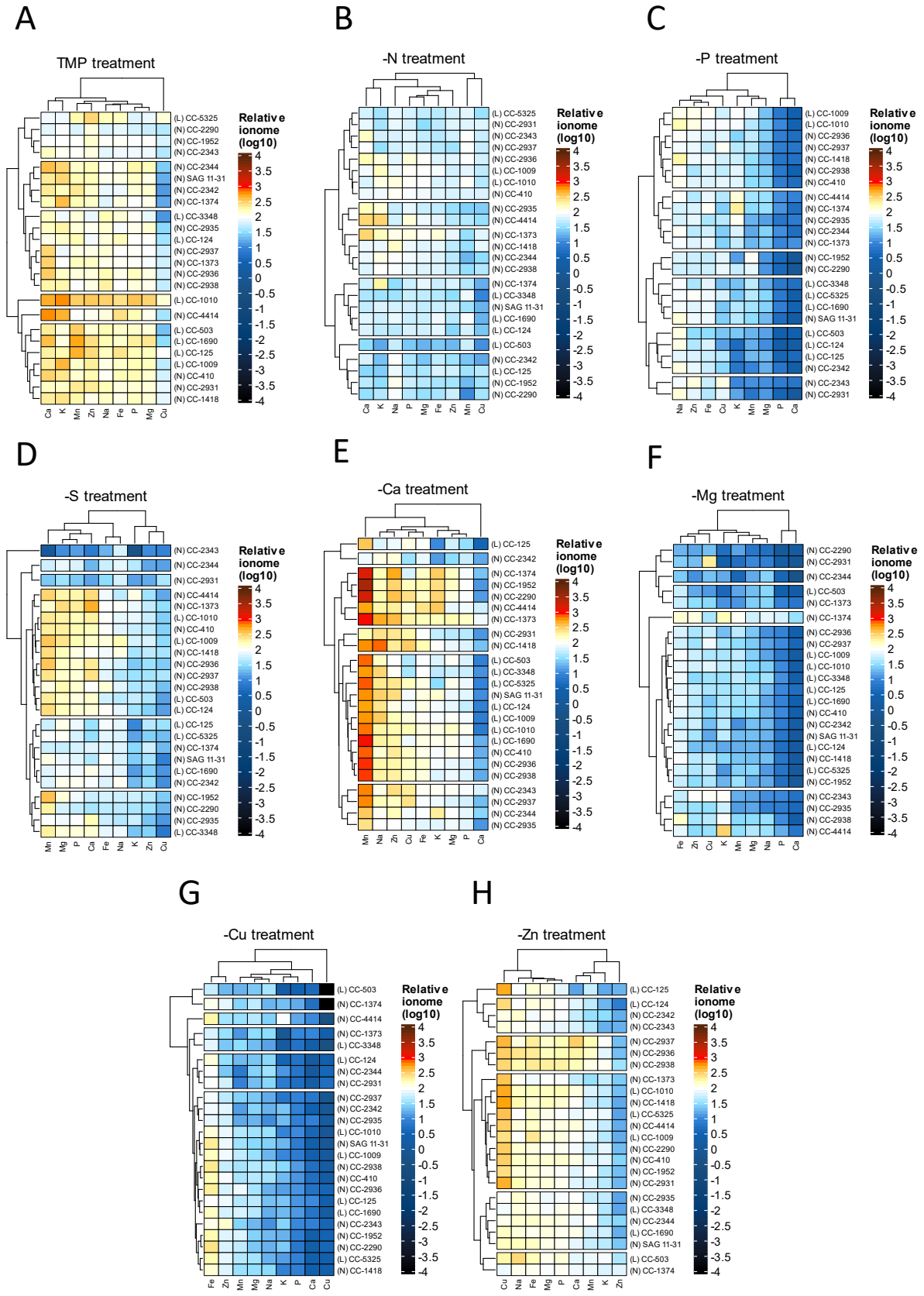

Figure S.II.6. Clustering of 24 Chlamydomonas strains based on their ionome profiles. The concentrations of 9 elements (Ca, Cu, Fe, K, Mg, Mn, Na, P, Zn) were measured by ICP-AES in samples collected at day 4 of culture in TMP **(A)** and in TAP -N **(B)**, -P **(C)**, -S **(D)**, -Ca **(E)**, -Mg **(F)**, -Cu **(G)** and -Zn **(H)**. Concentration values are provided as mean values from 2 independent experiments, with 2 replicates each (n=4). For easier representation, null values were replaced by 10^{-4}. The data was scaled using a $\log_{10}$ transformation and the control value, represented as 2 (100% = [10^2] %), is coloured white. Dendrograms represent the Euclidean distance clustered by complete linkage. Strain origin [natural (N) or laboratory (L)] is shown between brackets.

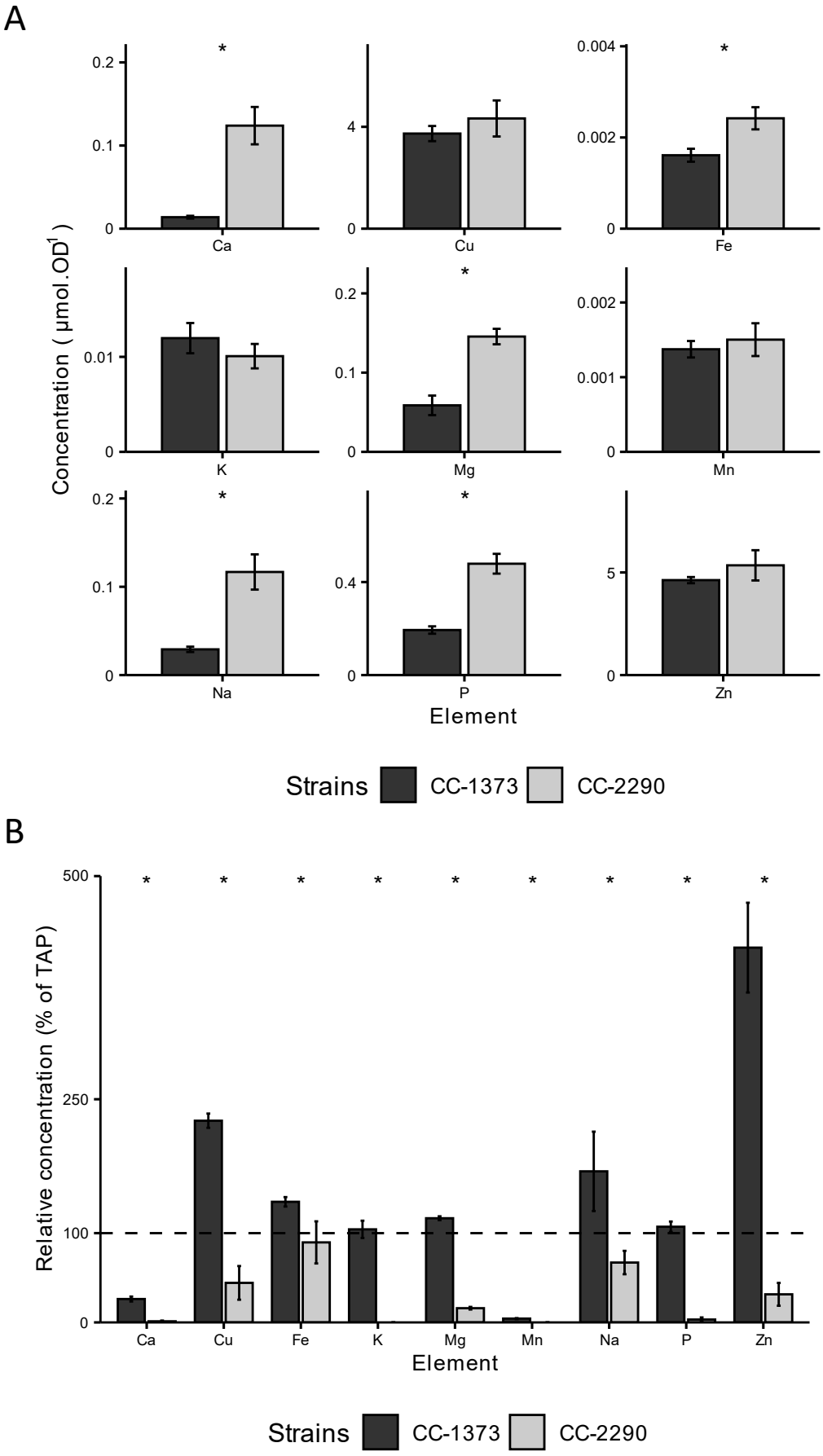

Figure S.II.7. Comparison of the nutrient concentrations in the CC-1373 and CC-2290 natural Chlamydomonas strains upon Mn deficiency. Samples were analyzed by ICP-AES at day 4 of culture (A) in TAP control media (µmol. OD-1) and (B) in –Mn (% of TAP control media). Significant differences ($p<0.05$) are marked with a *.

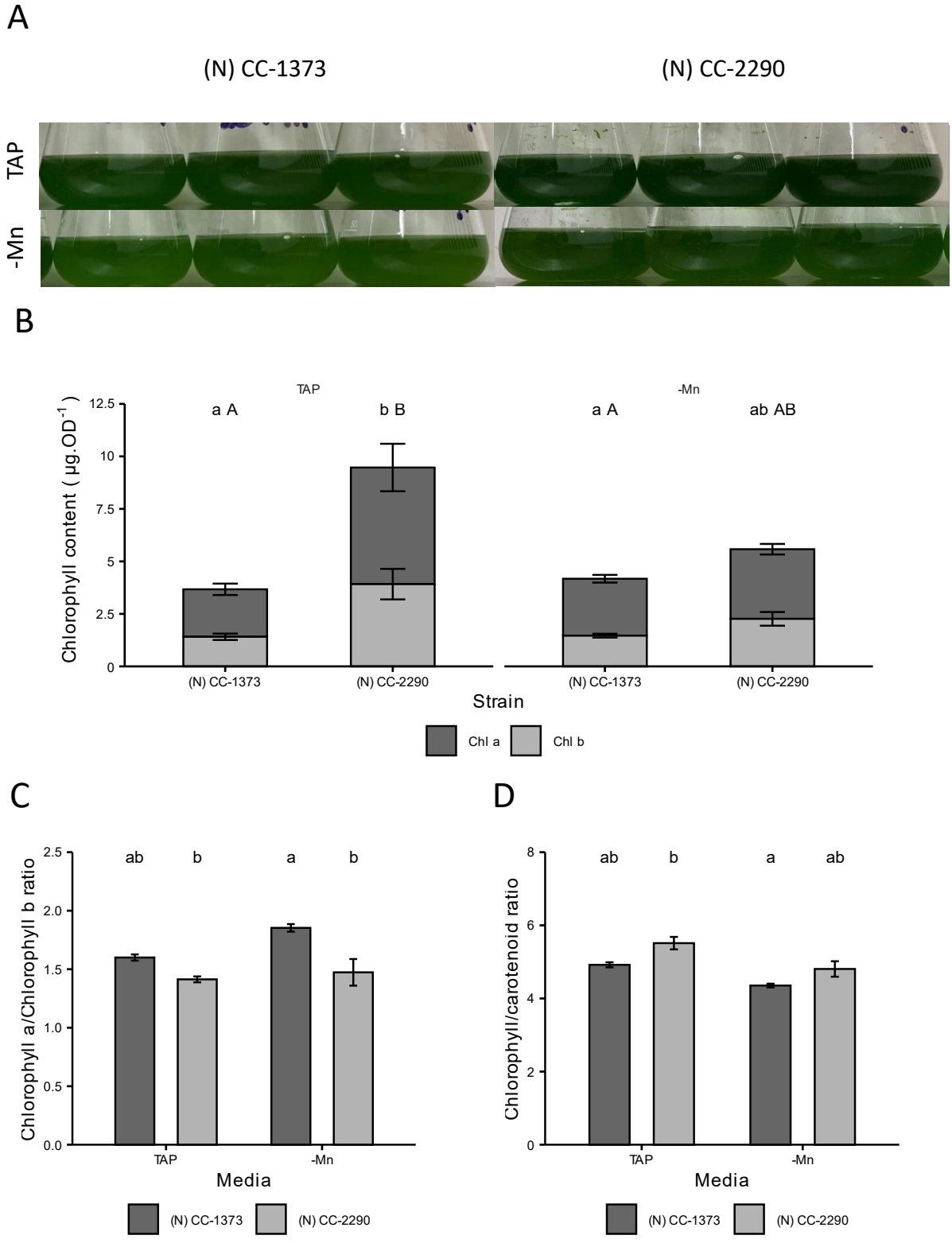

Figure S.II.8 Variation of the pigment composition in response to Mn deficiency between the CC-1373 and CC-2290 Chlamydomonas natural strains. (A) Natural strains CC-1373 (left) and CC-2290 (right) at day 4 of growth in TAP (top) and TAP -Mn (bottom). (B) Content in chlorophylls a (dark grey) and b (light grey). (C) Ratio between chlorophyll a and chlorophyll b. (D) Ratio between chlorophylls (a and b) and carotenoids. (B-D). Values are means ± SD (n=3). Non-parametric pairwise multiple comparisons were performed using Dunn's test and the different grouping letter were attributed when statistical differences were found. Small letter in (B) refer to the initial Fv/Fm while the capital letters refer to the recovery.

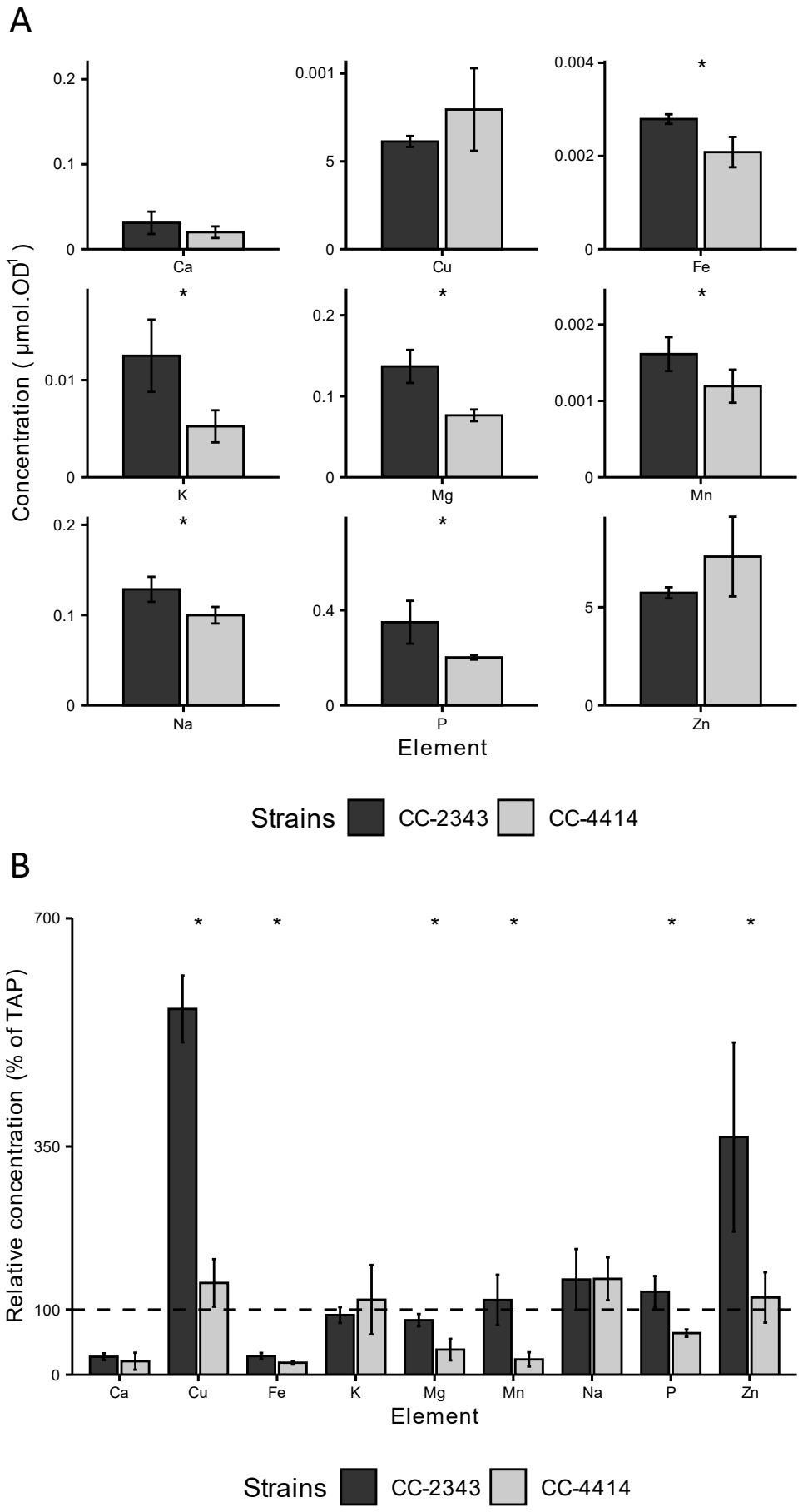

Figure S.II.9. Comparison of the nutrient concentrations in the CC-2343 and CC-4414 natural Chlamydomonas strains upon Fe deficiency. Samples were analyzed by ICP-AES at day 4 of culture (A) in TAP control media (µmol. OD-1) and (B) in –Fe (% of TAP control media). Significant differences ($p<0.05$) are marked with a *.

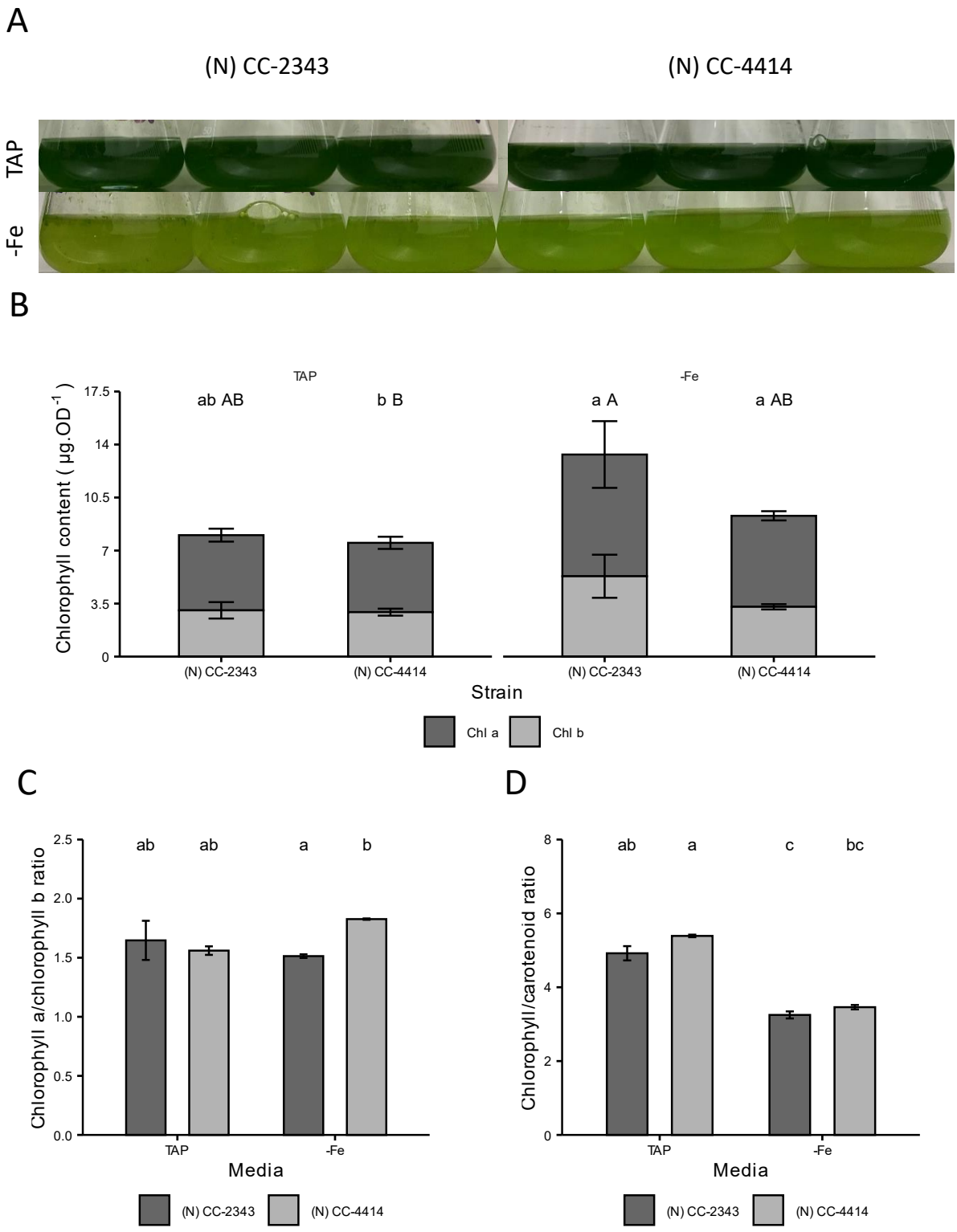

Figure S.II.10. Variation of the pigment composition in response to Fe deficiency between the CC-2343 and CC-4414 Chlamydomonas natural strains. (A) Natural strains CC-2343 (left) and CC-4414 (right) at day 4 of growth in TAP (top) and TAP-Fe (bottom). (B) Content in chlorophylls a (dark grey) and b (light grey). (C) Ratio between chlorophyll a and chlorophyll b. (D) Ratio between chlorophylls (a and b) and carotenoids. (B-D). Values are means ± SD (n=3). Non-parametric pairwise multiple comparisons were performed using Dunn's test and the different grouping letter were attributed when statistical differences were found. Small letter in (B) refer to the initial Fv/Fm while the capital letters refer to the recovery.

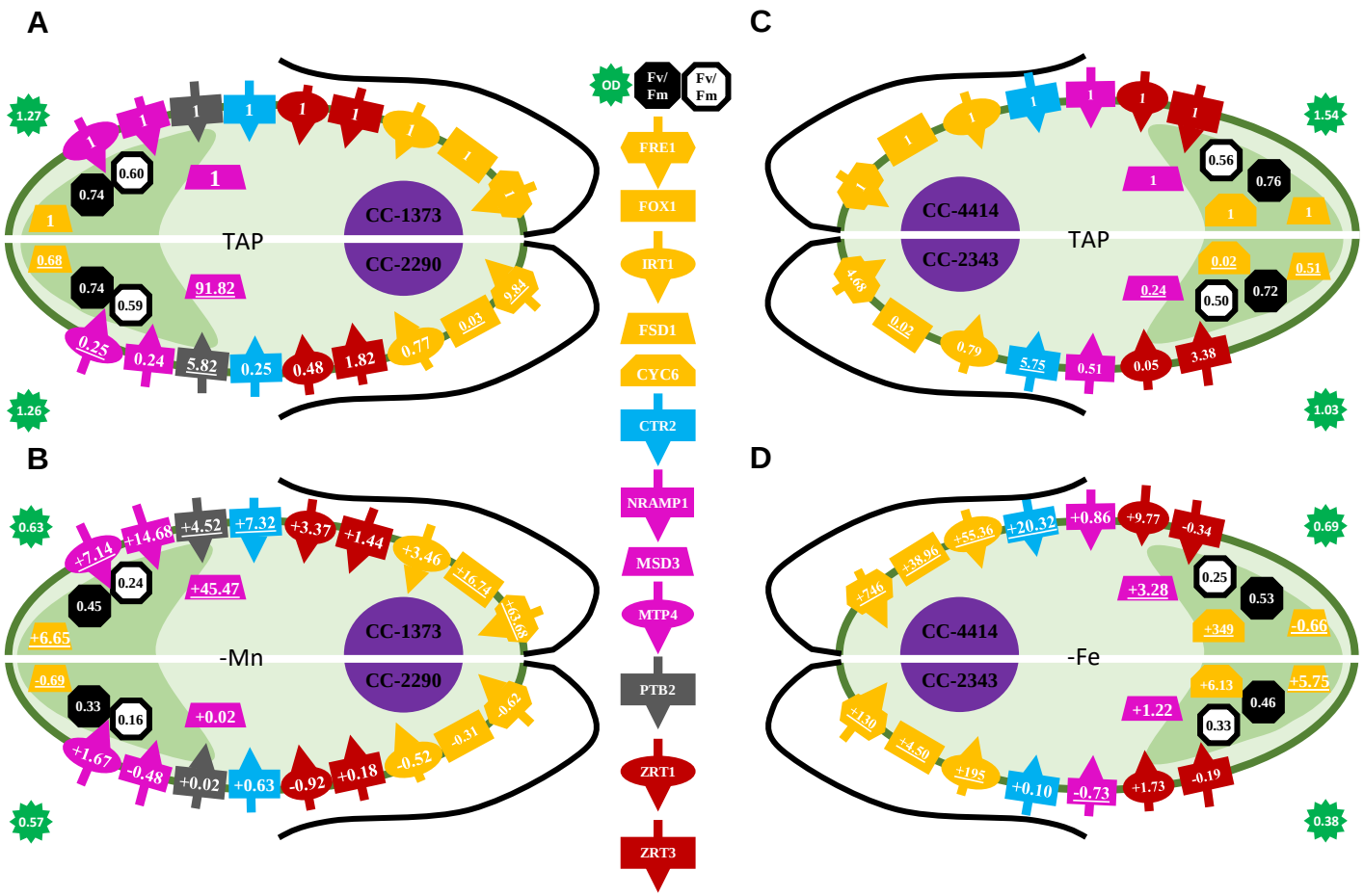

Figure S.II.11. Summary scheme of marker gene expression and photosynthesis variations among selected pairs of natural strains. (A-B) Strains CC-1373 and CC-2290 in control condition (A) and under -Mn (B). (C-D) Strains CC-4414 and CC-2343 in control condition (C) and under -Fe (D). The colored shapes indicate different gene markers (metal transporters represented with an arrow), color-coded according to the associated metal (yellow: iron, blue: copper, pink: manganese, grey: phosphate, red: zinc. Hexagons represent the Fv/Fm after dark adaptation (black) and after 23 minutes of saturating light (white). Stars represent the average OD750nm at day 4 of culture.

Table S.II.1. Description of the 24 Chlamydomonas strain panel.

Identifier	Additional information	Source
CC-124	agg1 allele, wild type mt- [137c]	https://www.chlamycollection.org/product/cc-124-wild-type-mt-137c/
CC-125	agg1+ allele, wild type mt+ [137c]	https://www.chlamycollection.org/product/cc-125-wild-type-mt-137c/
CC-410	wild type mt- [SAG 11-32c, Lewin Caroline Islands strain; really 137c	https://www.chlamycollection.org/product/cc-410-wild-type-mt-sag-11-32c-lewin-caroline-islands-strain-really-137c/
CC-503	Wall deficient, cw92 mt+	https://www.chlamycollection.org/product/cc-503-cw92-mt/
CC-1009	Can grow on nitrate, wild type mt- [UTEX 89]	https://www.chlamycollection.org/product/cc-1009-wild-type-mt-utex-89 /
CC-1010	Can grow on nitrate, wild type mt+ [UTEX 90]	https://www.chlamycollection.org/product/cc-1010-wild-type-mt-utex-90/
CC-1373	C. smithii mt+ [SAG 54.72]	https://www.chlamycollection.org/product/cc-1373-c-smithii-mt-sag-54-72/
CC-1374	mt+ [SAG 77.81]	https://www.chlamycollection.org/product/cc-1374-c-reinhardtii-sag-77-81/
CC-1418	mt- [SAG 18.79]	https://www.chlamycollection.org/product/cc-1418-c-reinhardtii-mt-sag-18-79/
CC-1690	wild type mt+ [Sager 21 gr]	https://www.chlamycollection.org/product/cc-1690-wild-type-mt-sager-21-gr/
CC-1952	Can grow on nitrate, S1 C5 mt-	https://www.chlamycollection.org/product/cc-1952-c-reinhardtii-mt-s-1-c-5/
CC-2290	Can grow on nitrate, S1 D2 mt-	https://www.chlamycollection.org/product/cc-2290-s1-d2-mt/
CC-2342	Can grow on nitrate, wild type mt- [Jarvik #6, Pittsburgh, PA]	https://www.chlamycollection.org/product/cc-2342-wild-type-mt-jarvik-6-pittsburgh-pa/
CC-2343	Can grow on nitrate, wild type mt+ [Jarvik #224, Melbourne, FL]	https://www.chlamycollection.org/product/cc-2343-wild-type-mt-jarvik-224-melbourne-fl/
CC-2344	Can grow on nitrate, wild type mt+ [Jarvik #356, Ralston, PA]	https://www.chlamycollection.org/product/cc-2344-wild-type-mt-jarvik-356-ralston-pa/
CC-2931	lack the Gulliver transposon, wild type mt- [North Carolina]	https://www.chlamycollection.org/product/cc-2931-wild-type-mt-north-carolina/
CC-2935	Bell's isolate LEE-1, wild type mt- [Quebec]	https://www.chlamycollection.org/product/cc-2935-wild-type-mt-quebec/
CC-2936	Bell's isolate LEE-2, wild type mt- [Quebec]	https://www.chlamycollection.org/product/cc-2936-wild-type-mt-quebec/
CC-2937	Bell's isolate LEE-3, wild type mt+ [Quebec]	https://www.chlamycollection.org/product/cc-2937-wild-type-mt-quebec/
CC-2938	Bell's isolate LEE-4, wild type mt+ [Quebec]	https://www.chlamycollection.org/product/cc-2938-wild-type-mt-quebec/
CC-3348	wild type mt+ [SAG 73.72, = C8]	https://www.chlamycollection.org/product/cc-3348-wild-type-mt-sag-73-72-c8/
CC-4414	can grow at low temperatures, wild type mt+ DN2	https://www.chlamycollection.org/product/cc-4414-wild-type-mt-dn2/
CC-5325	thawed from cryogenic storage, cw15 mt-	https://www.chlamycollection.org/product/cc-5325-cw15-mt-jonikas-cmj030-jr397/
SAG 11-31	Good survival to cryopreservation, mt+	https://sagdb.uni-goettingen.de/detailedList.php?str_number=11-31

The 10 laboratory strains are underlined. CC: Chlamydomonas Center; SAG: Sammlung von Algenkulturen der Universität Göttingen (Göttingen University Culture Collection of Algae).

Table S.II.2. Composition of the single element deficiency TAP media.

Nutrient	Condition	TAP Control (μM)	Deficiency (μM)	Ratio
		Macronutrients		
Acetate (CH_3COOH)	TMP	17,416	0	0
Calcium	-Ca	387.6	0	0
Magnesium	-Mg	405.7	5.4	$^1/_{75}$
Nitrogen	-N	7478	747.9	$^1/_{10}$
Sulphur	-S	506.5	56.6	$^1/_{9}$
Phosphate	-P	1000	100	$^1/_{10}$
		Micronutrients		
Iron	-Fe	17.95	1.8	$^1/_{10}$
Copper	-Cu	6.29	0.006	$^1/_{1000}$
Manganese	-Mn	25.6	0	0
Zinc	-Zn	76.5	0	0

Table S.II.3. Deficiency marker gene description and RT-qPCR primers.

Gene	Gene ID (v5)	Name & Description	Primer sequences (5' - 3')	Length	Product length	Efficiency	Reference	Condition
RPL13 (R)	Cre14.g630100	Ribosomal protein L13, component of cytosolic 80S ribosome and 60S large subunit	TCAGCGTCTGAAGGCTTACC CTCGGCCAGAGGGGTCTCGA	20 20	88	1.91	Durante et al., 2019	TAP -Mn, -Fe
CBLP (R)	Cre06.g278222	Receptor of activated protein kinase C	GTGTCGTGCGTGCGCTTCT CACCAGGTTGTTCTTCAGCTTGC	19 23	117	1.93	Durante et al., 2019	TAP -Mn, -Fe
CTR2	Cre10.g434350	CTR type copper ion transporter	CACCAACAGCCTTTCCACAAG GACGCTGAACTGCGTAACCT	21 20	94	1.92	Allen et al., 2007b	TAP -Mn, -Fe
CYC6	Cre16.g651050	Cytochrome C oxidase, cbb3-type, subunit III. Cytochrome c6	AGGCTTGGGCCAGTACATTA GTGCAAAACCCGGTTGAAGC	20 20	150	1.92	Quinn & Merchant 1995	TAP -Fe
IRT1	Cre12.g530400	Iron Regulated Transporter1. Iron-nutrition responsive ZIP family transporter	CACAGTAGGGGCATGAGAGC CCCAATCCCAGTCCGTTAGG	20 20	81	1.90	Allen et al., 2007a Allen et al., 2007b	TAP -Mn, -Fe
FOX1	Cre09.g393150	Ferroxidase 1. Multicopper ferroxidase	TTGCGCTGCATGCAATAAGG GTTCGCGGCTCAACACAAAA	20 20	141	1.93	Allen et al., 2007a	TAP -Mn, -Fe
FRE1	Cre04.g227400	Ferric-chelate reductase/ oxidoreductase. Ferrireductase	CACTTCGCCAAGGACTCCAG GGGTCCAGGCATTGTACTTCT	20 21	124	1.915	Allen et al., 2007a	TAP -Mn, -Fe
FSD1	Cre10.g436050	Fe superoxide dismutase	CATGAACAAGCAGGTCGCTG GGCTTCATGCTCTCCCAGAA	20 20	150	1.91	Allen et al., 2007b	TAP -Mn, -Fe
MSD3	Cre16.g676150	Mn superoxide dismutase	GGACGCAATGCTGTGCTAAG TCTTGTCCGCAAAGCCTCAT	20 20	115	1.93	Allen et al., 2007b	TAP -Mn, -Fe
MTP4	Cre03.g160550	Metal Transport Protein (CDF transporter). Cation efflux transporter, membrane protein	CGTGATGAAGCCACTGCCTA CGATCTTGTCCCCCTCCTTT	20 20	108	1.92	Allen et al., 2007b	TAP -Mn
NRAMP1	Cre17.g707700	Natural Resistance Associated Macrophage-like Protein 1. Manganese/metal transporter, NRAMP homolog	GCGGGTAATCCAGGGCTTTT GGAACCACCAGAGTGCAAGT	20 20	92	1.90	Allen et al., 2007b	TAP -Mn, -Fe
PTB2	Cre07.g325741	Phosphate transporter. Sodium/phosphate symporter	CTGCCCATGACCTTCAACCA GAAGTCAGCAACGCTTTCCC	20 20	145	1.90	Allen et al., 2007b	TAP -Mn
ZRT1	Cre07.g351950	Zn Regulator Transporter 1. Zinc-nutrition responsive transporter	CATTCTCAGTGCTCGCGTTG GAGCGCCACCTCTTCCTTAG	20 20	88	1.91	Allen et al., 2007b	TAP -Mn, -Fe
ZRT3	Cre13.g573950	Zinc-nutrition responsive transporter	GCGGCATTAATAGCGCTGAA CCGCCTACTTCCTGGTTTCT	20 20	86	1.96	Allen et al., 2007b	TAP -Mn, -Fe

v5: JGI v5 annotation of the genome (https://phytozome-next.jgi.doe.gov/info/Creinhardtii_v5_6#:~:text=Overview,different%20environments%20throughout%20the%20world.)

Supplemental Tables and Figures
Chapter III

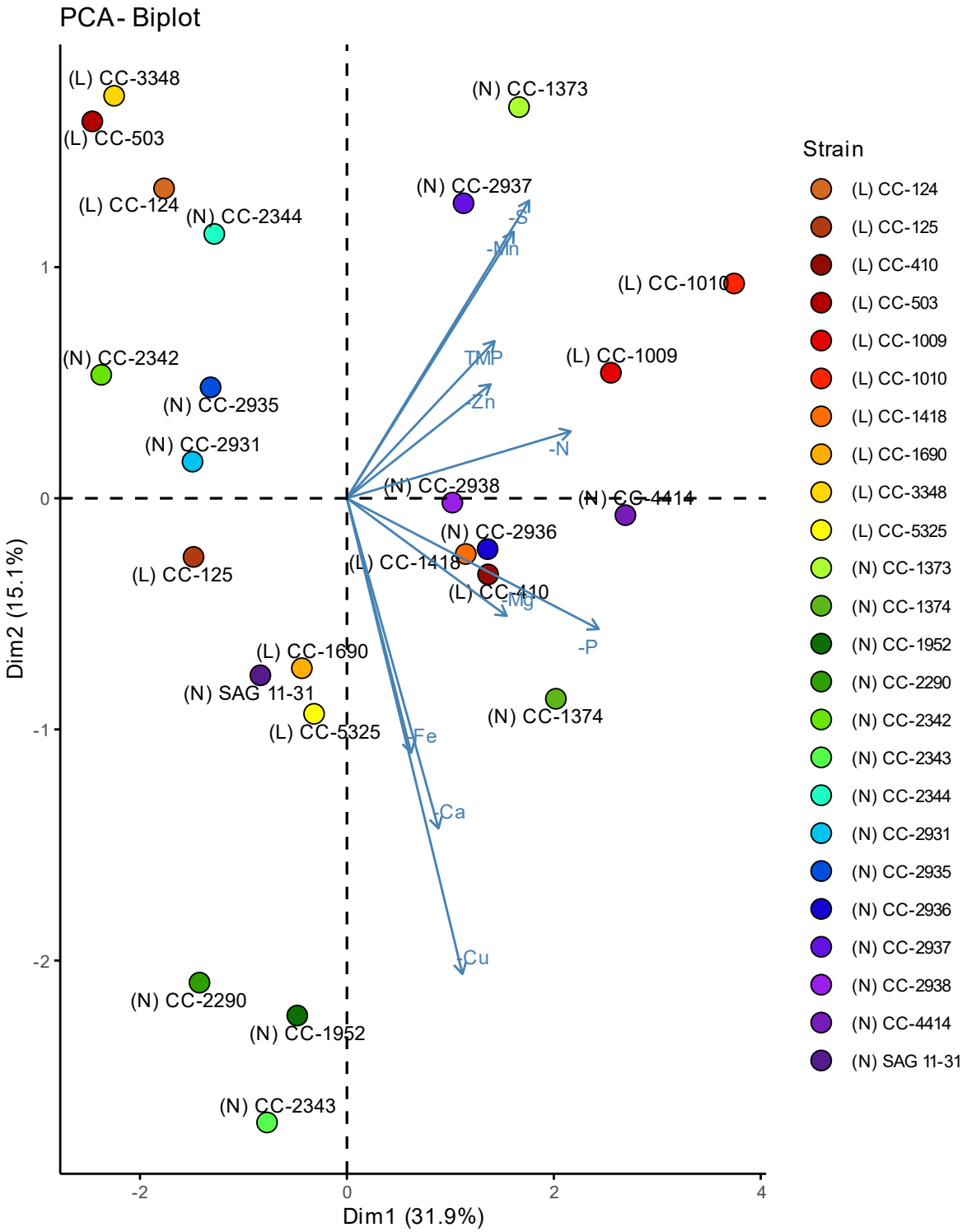

Figure S.III.1 Principal component analysis of the ionomic data of the 24 Chlamydomonas strains in response to nutrient deficiency. The strains were grown in 0 µM acetate (TMP), 0 µM Ca, 5.4 µM Mg, 2748 µM N, 56.6 µM S, 100 µM P, 1.8 µM Fe, 0.006 µM Cu, 0 µM Mn or 0 µM Zn. The 2 first dimensions explained 47% of the variation observed, and separated –S, -Mn, TMP and -Zn treatments (*top right*) from –P, -Mg, -Ca, -Fe and –Cu (*bottom right*).

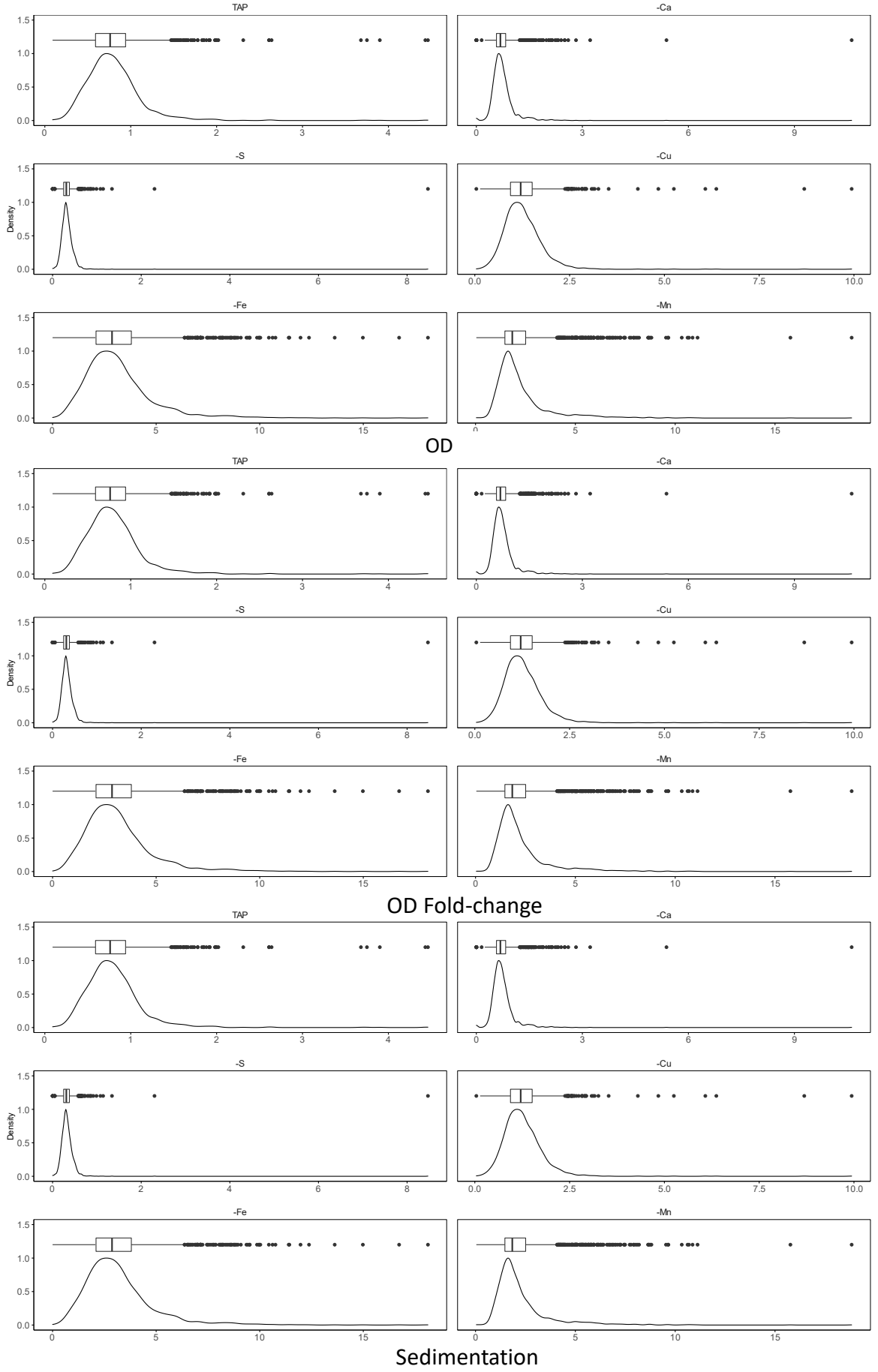

Figure S.III.2 Distribution of the biomass-related phenotypes of the MAGIC progeny in different media (TAP, TAP-Ca, -S, -Cu, -Fe and –Mn).

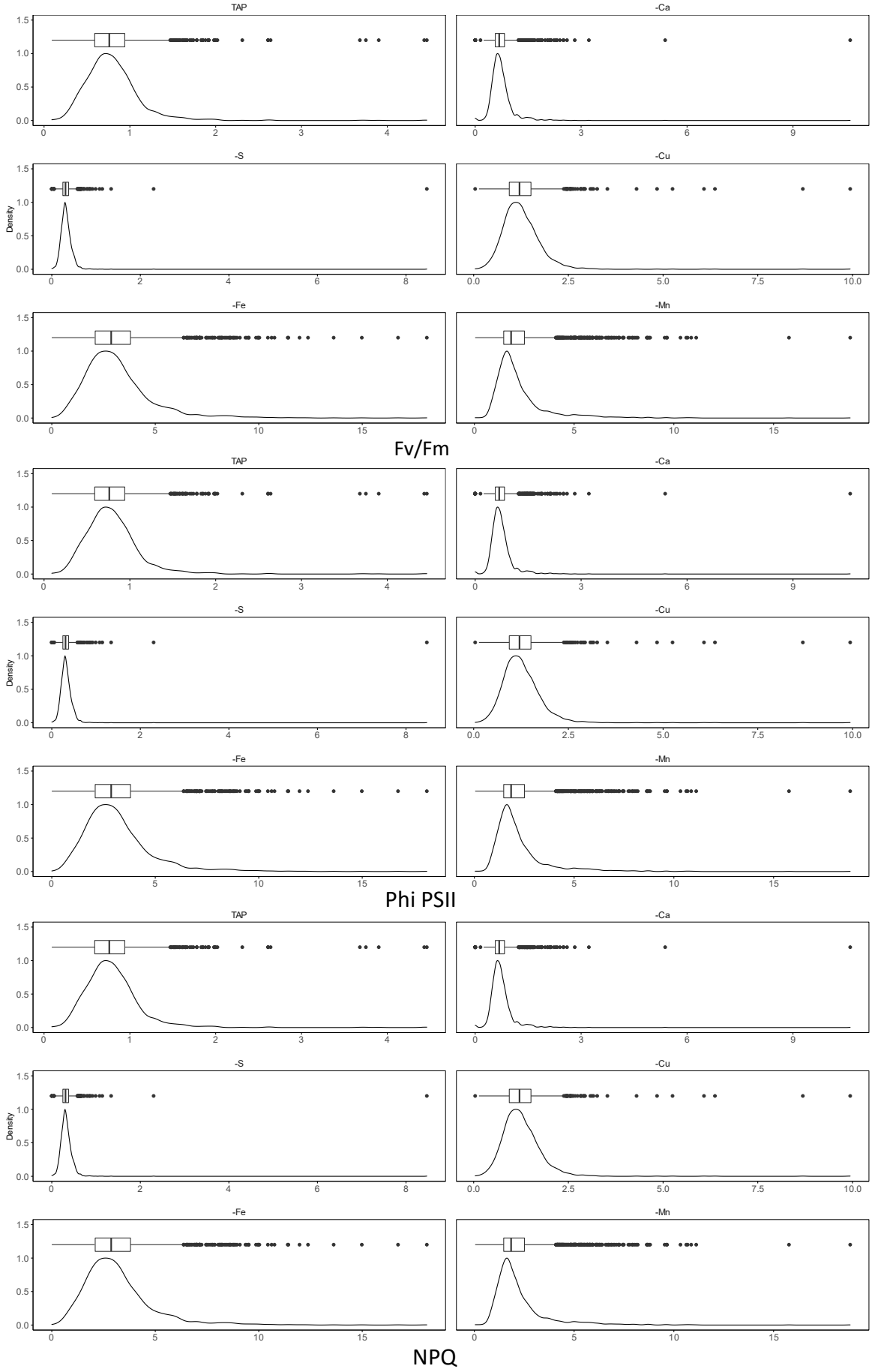

Figure S.III.3 Distribution of the photosynthesis-related phenotypes of the MAGIC progeny in different media (TAP, TAP-Ca, -S, -Cu, -Fe and –Mn).

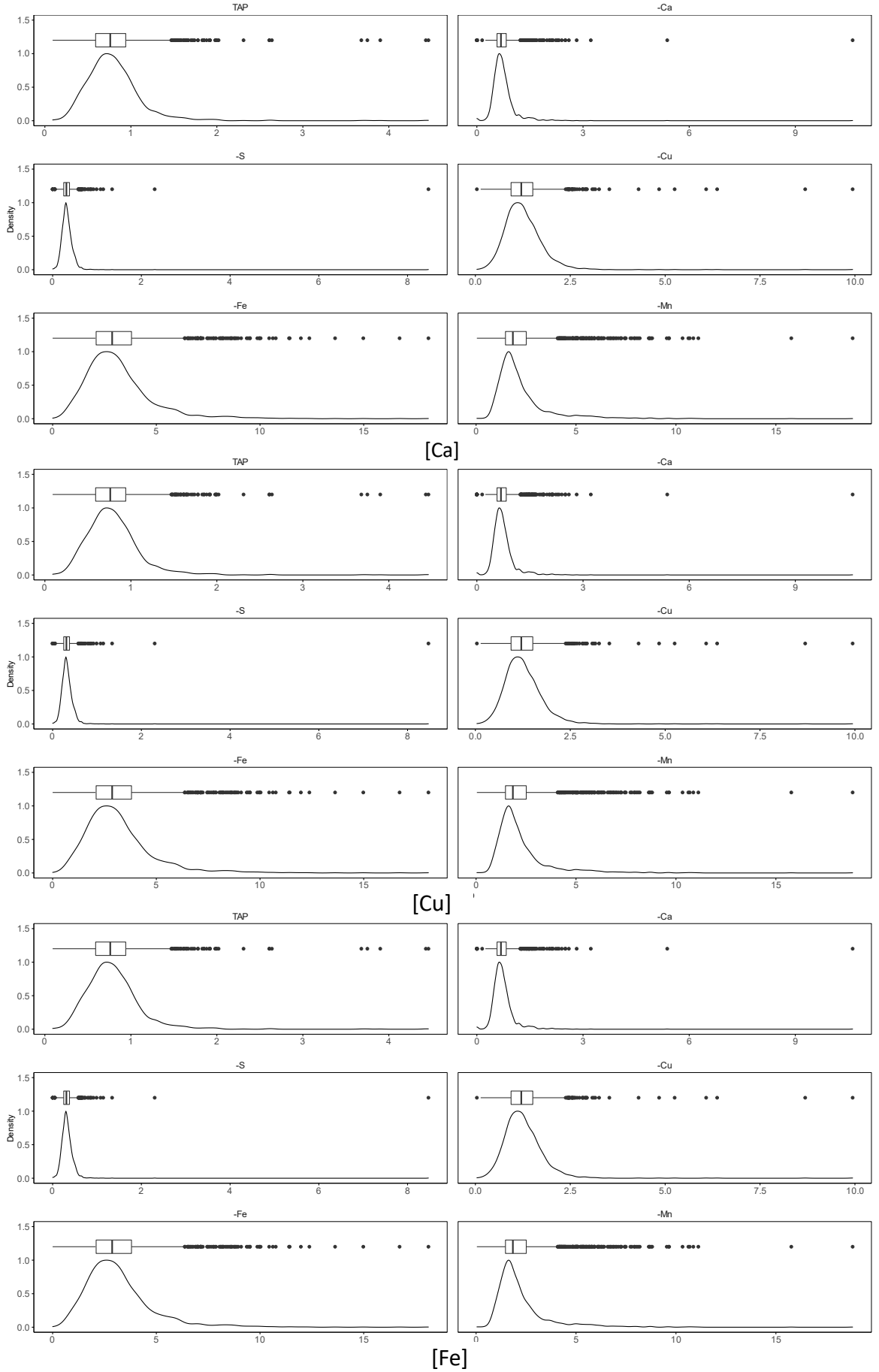

Figure S.III.4 Distribution of the Ca, Cu and Fe accumulation phenotypes of the MAGIC progeny in different media (TAP, TAP-Ca, -S, -Cu, -Fe and –Mn).

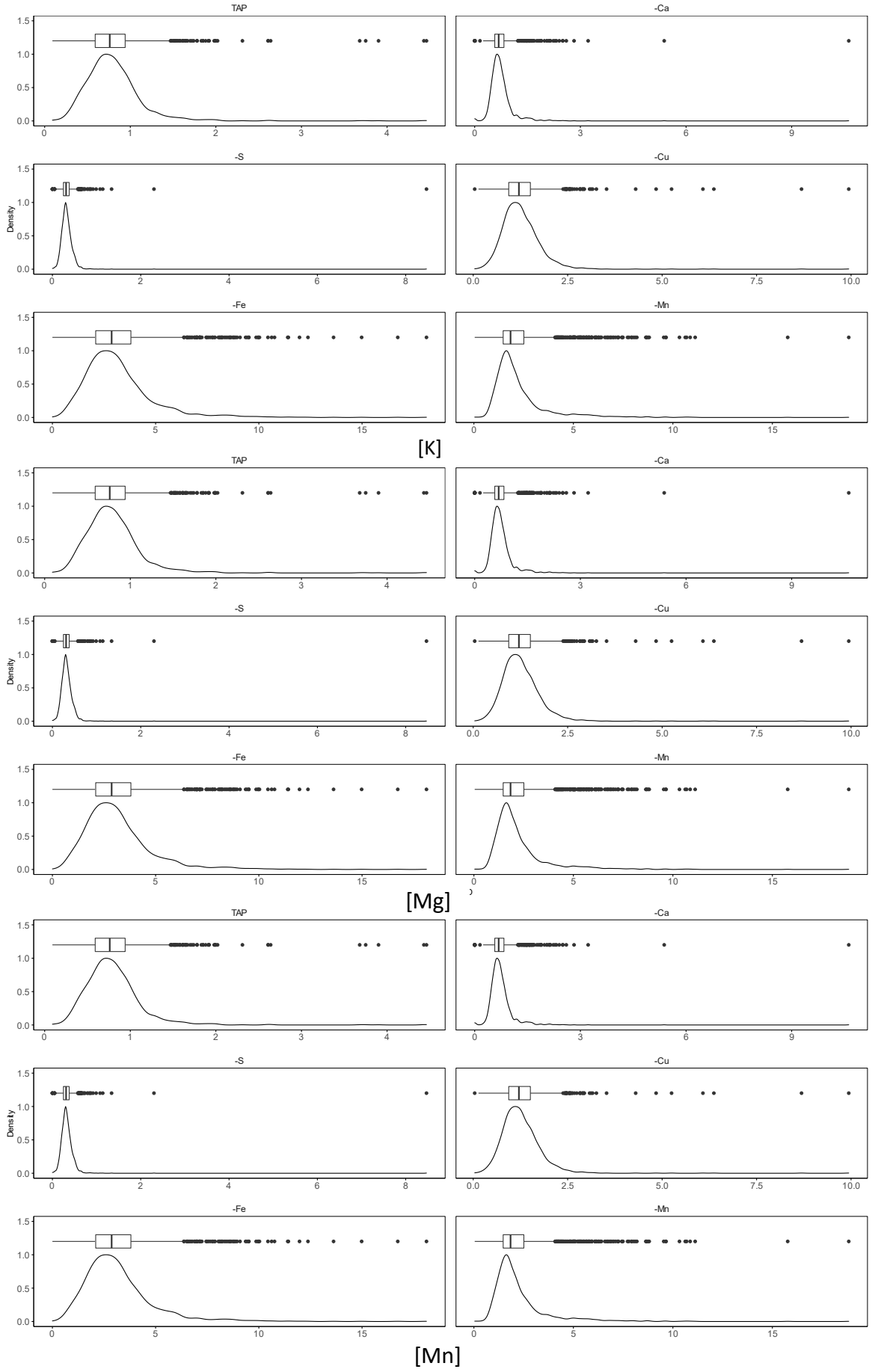

Figure S.III.5 Distribution of the K, Mg and Mn accumulation phenotypes of the MAGIC progeny in different media (TAP, TAP-Ca, -S, -Cu, -Fe and –Mn).

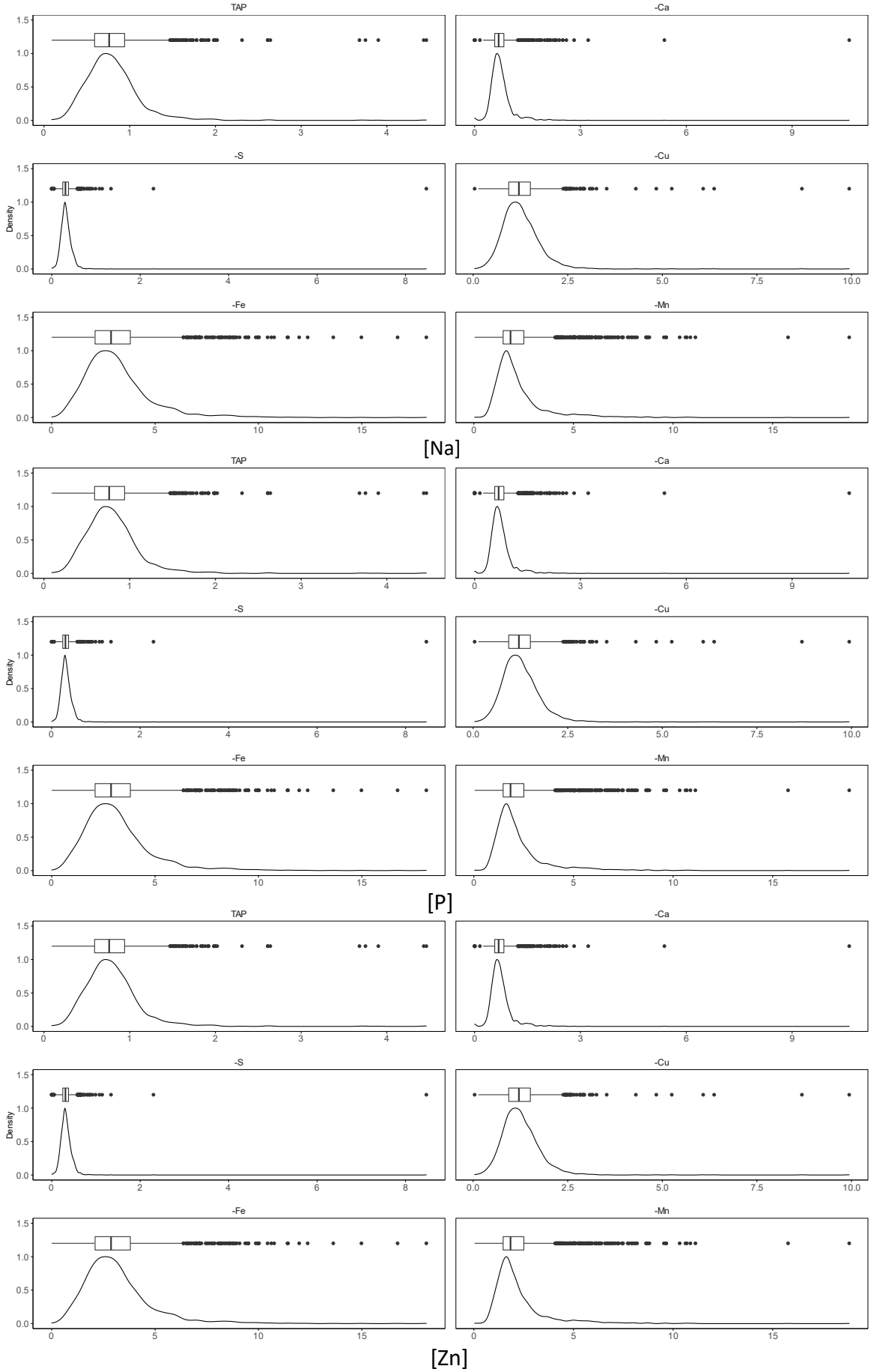

Figure S.III.6 Distribution of the Na, P and Zn accumulation phenotypes of the MAGIC progeny in different media (TAP, TAP-Ca, -S, -Cu, -Fe and –Mn).

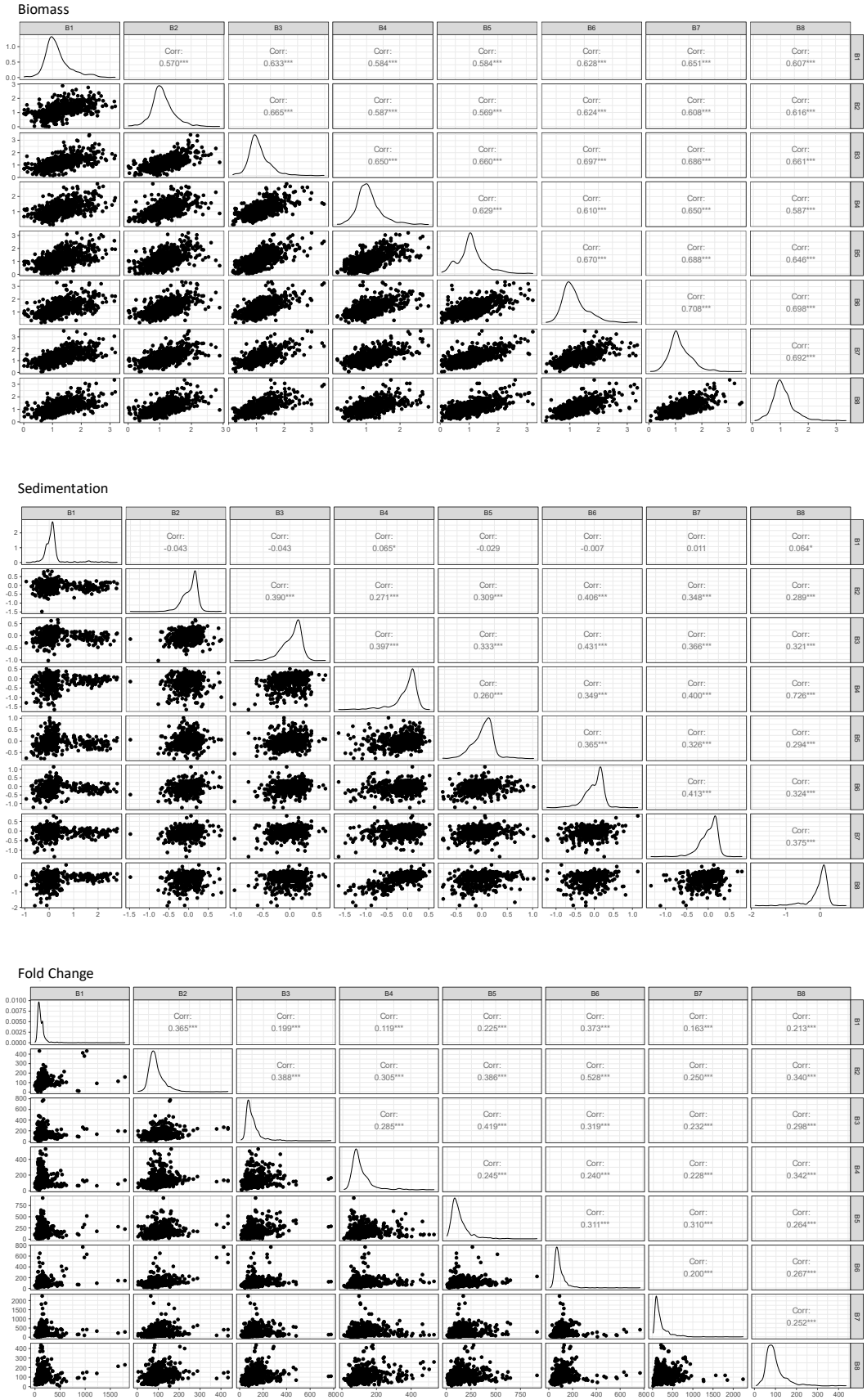

Figure S.III.7 Pairwise scatter plot matrix, histogram, and Pearson correlation coefficients between the 8 batches used to phenotype the MAGIC progeny (biomass-related traits). ******* if the p-value is < 0.001; ****** if the p-value is < 0.01; ***** if the p-value is < 0.05; **.** if the p-value is < 0.10

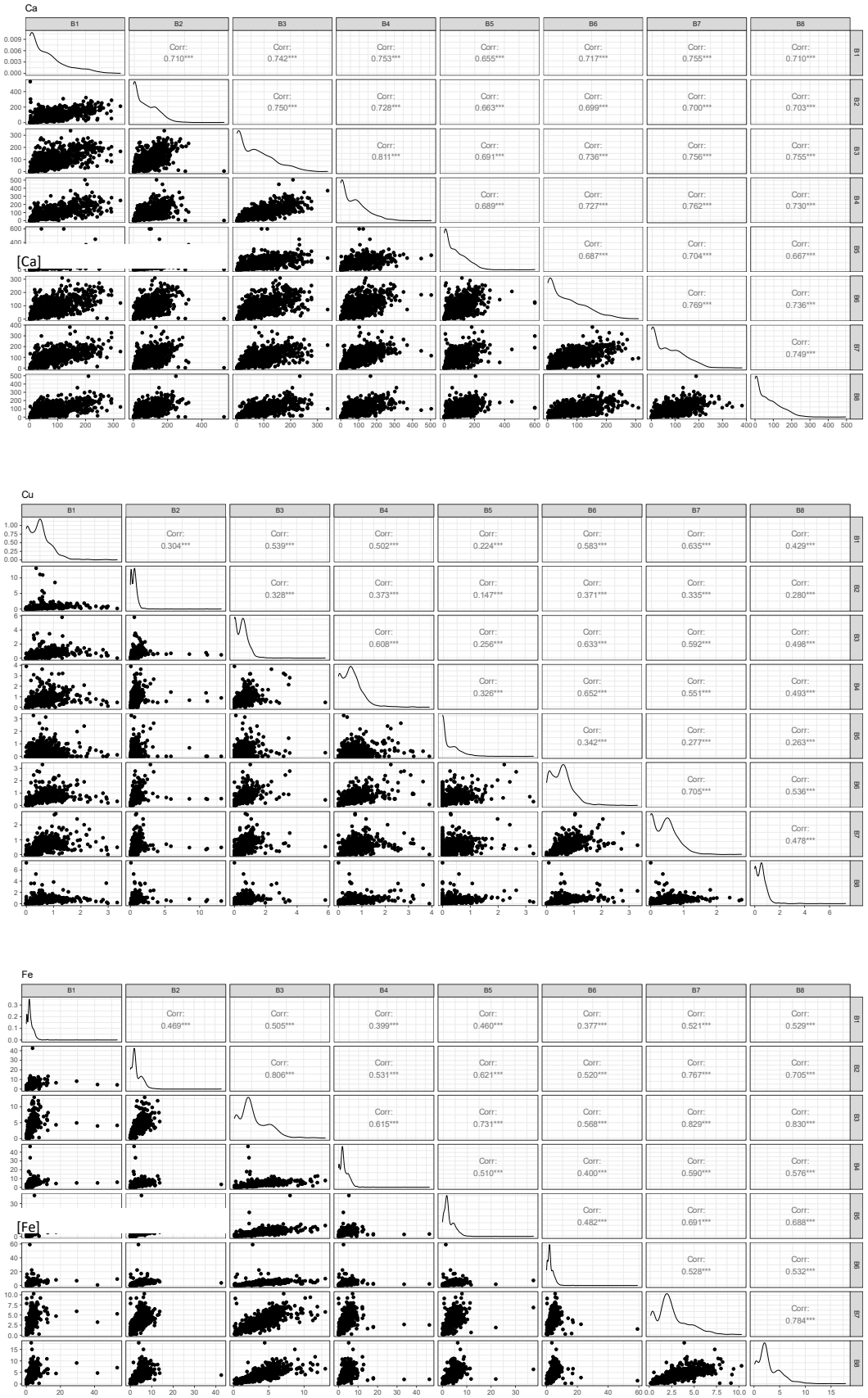

Figure S.III.8 Pairwise scatter plot matrix, histogram, and Pearson correlation coefficients between the 8 batches used to phenotype the MAGIC progeny ([Ca], [Cu], [Fe]).
******* if the p-value is < 0.001; ****** if the p-value is < 0.01; ***** if the p-value is < 0.05; **.** if the p-value is < 0.10

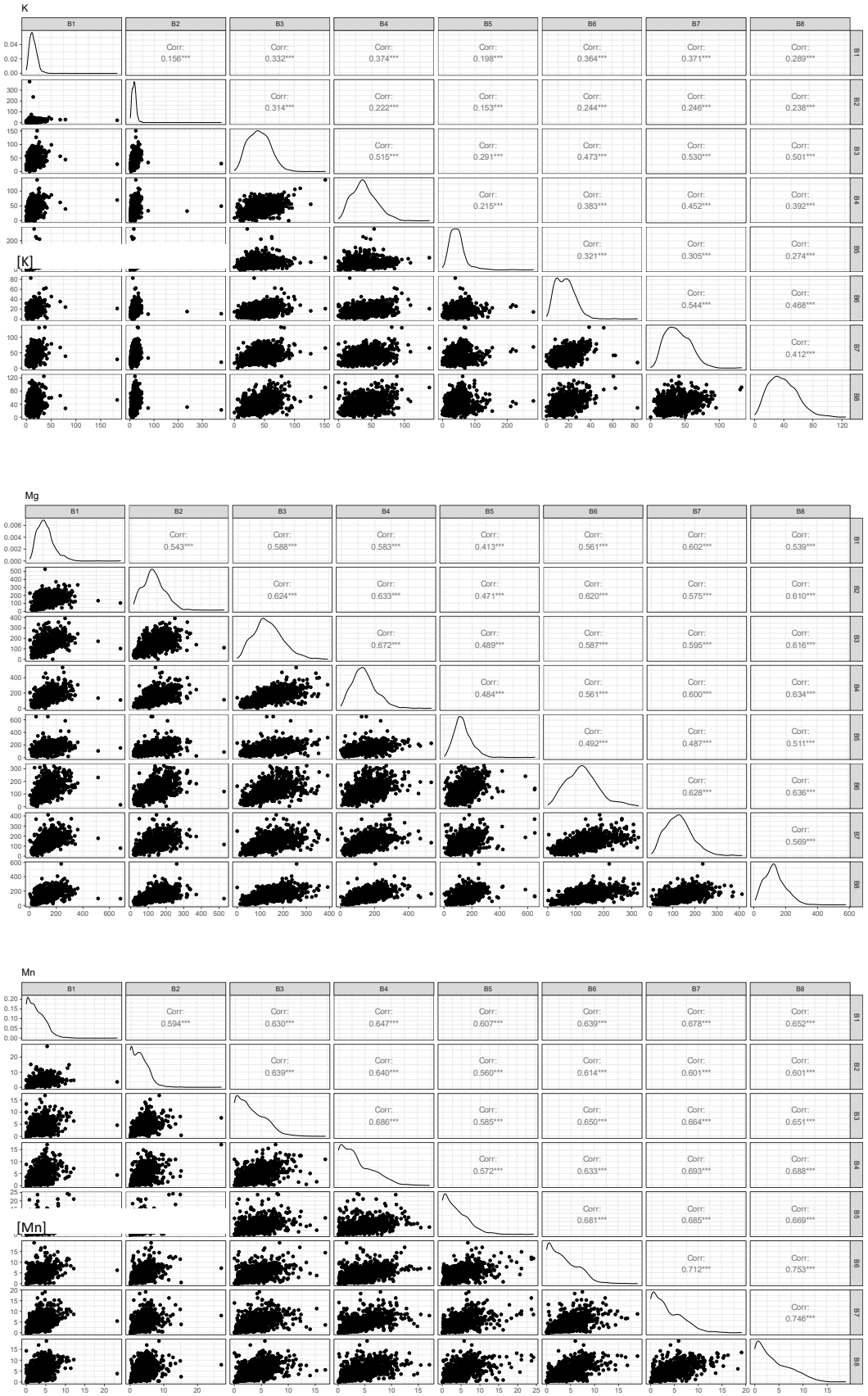

Figure S.III.9 Pairwise scatter plot matrix, histogram, and Pearson correlation coefficients between the 8 batches used to phenotype the MAGIC progeny ([K], [Mg], [Mn]).
******* if the p-value is < 0.001; ****** if the p-value is < 0.01; ***** if the p-value is < 0.05; **.** if the p-value is < 0.10

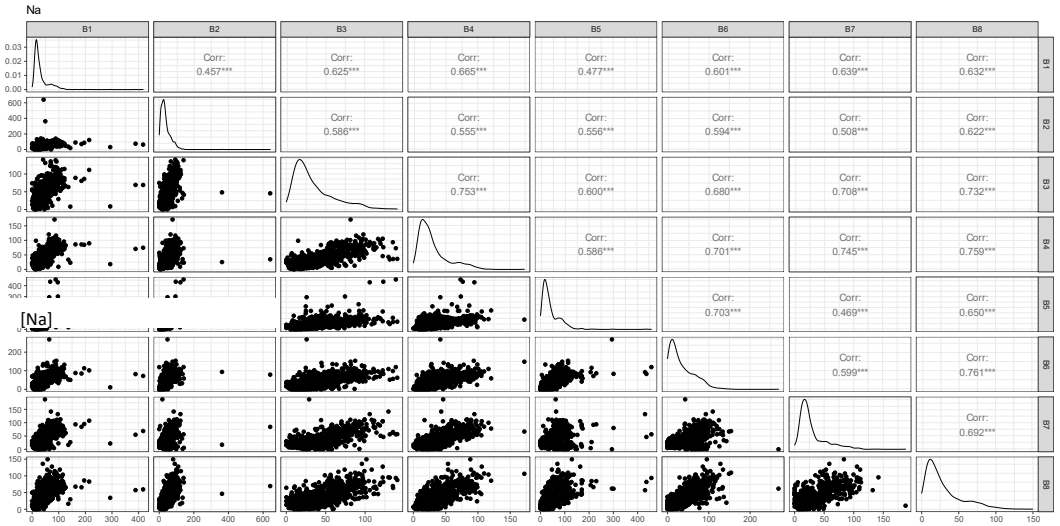

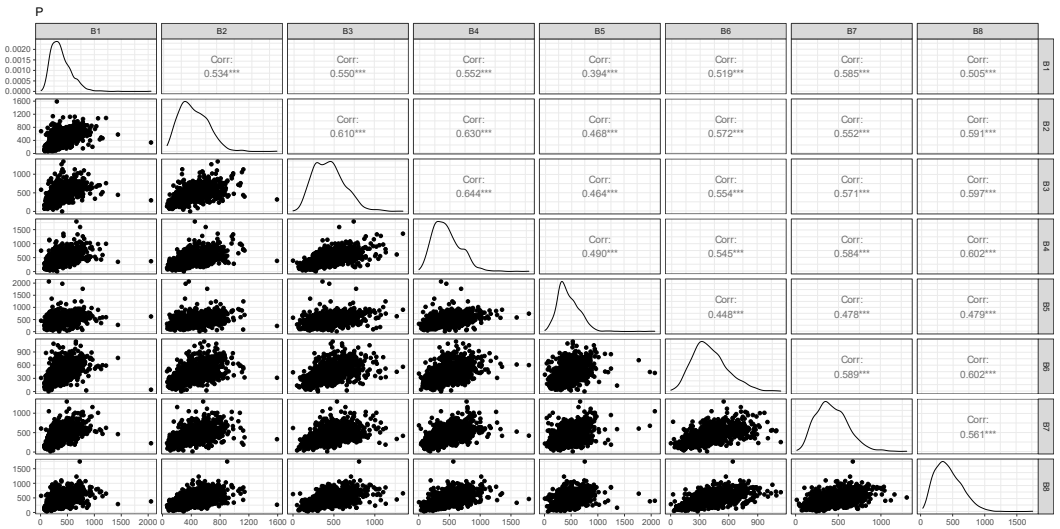

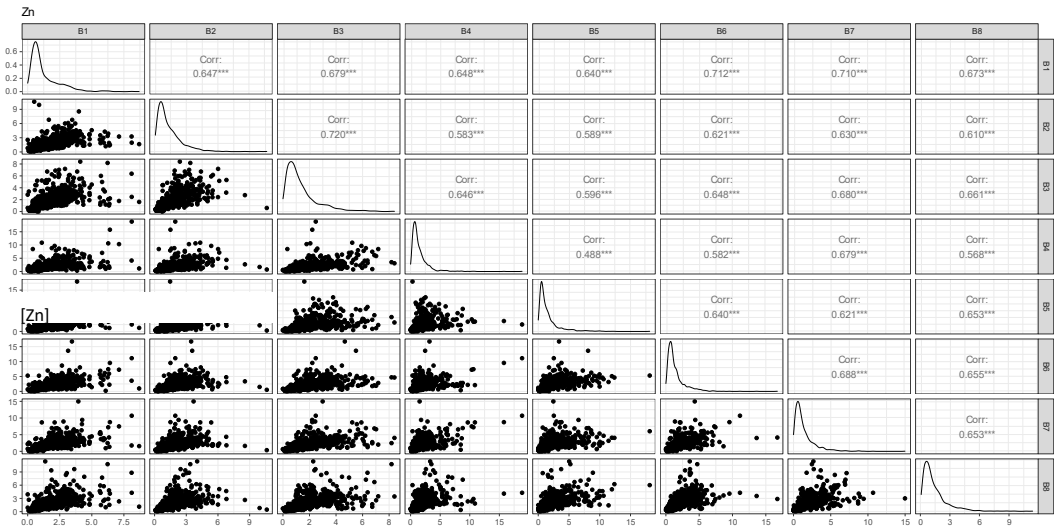

Figure S.III.10 Pairwise scatter plot matrix, histogram, and Pearson correlation coefficients between the 8 batches used to phenotype the MAGIC progeny ([Na], [P], [Zn]).
******* if the p-value is < 0.001; ****** if the p-value is < 0.01; ***** if the p-value is < 0.05; **.** if the p-value is < 0.10

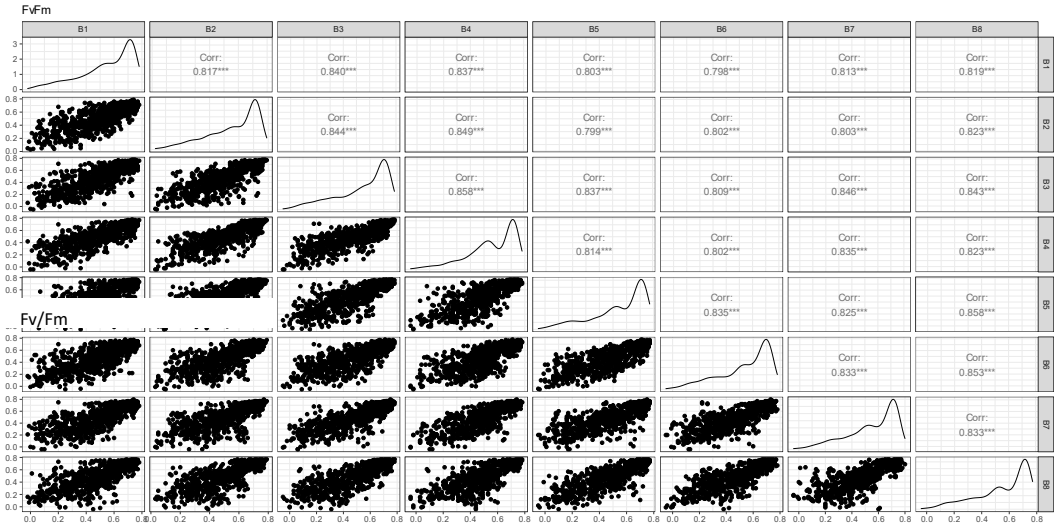

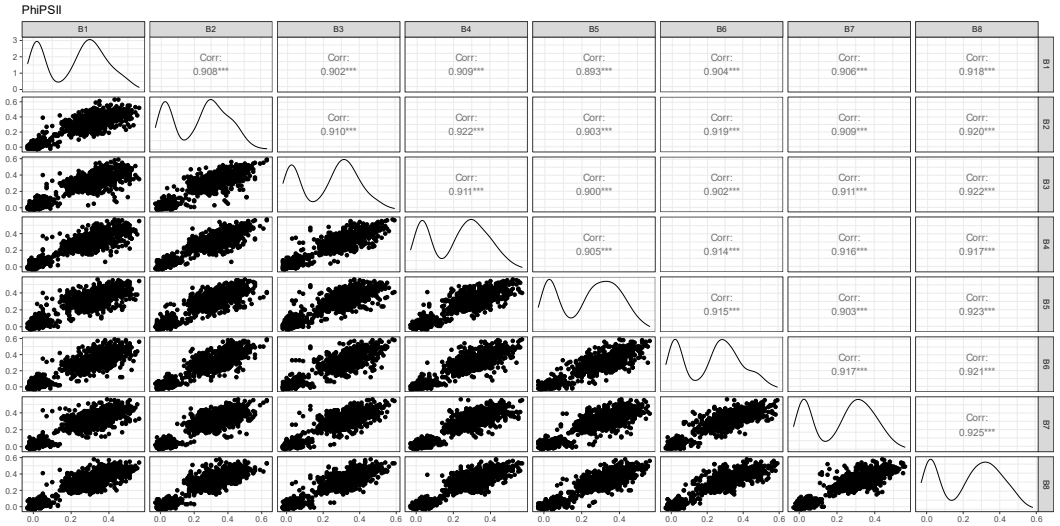

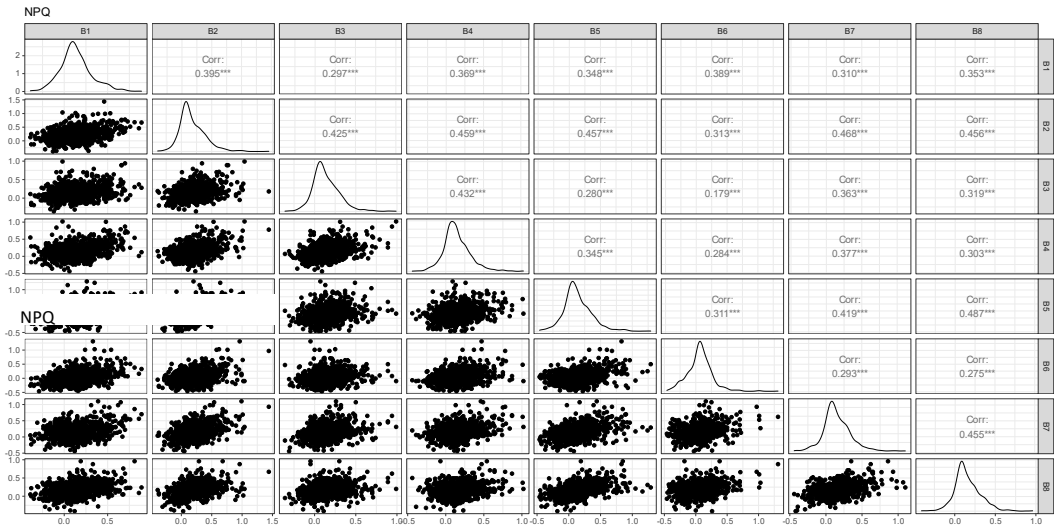

Figure S.III.11 Pairwise scatter plot matrix, histogram, and Pearson correlation coefficients between the 8 batches used to phenotype the MAGIC progeny (photosynthesis-related). ******* if the p-value is < 0.001; ****** if the p-value is < 0.01; ***** if the p-value is < 0.05; **.** if the p-value is < 0.10

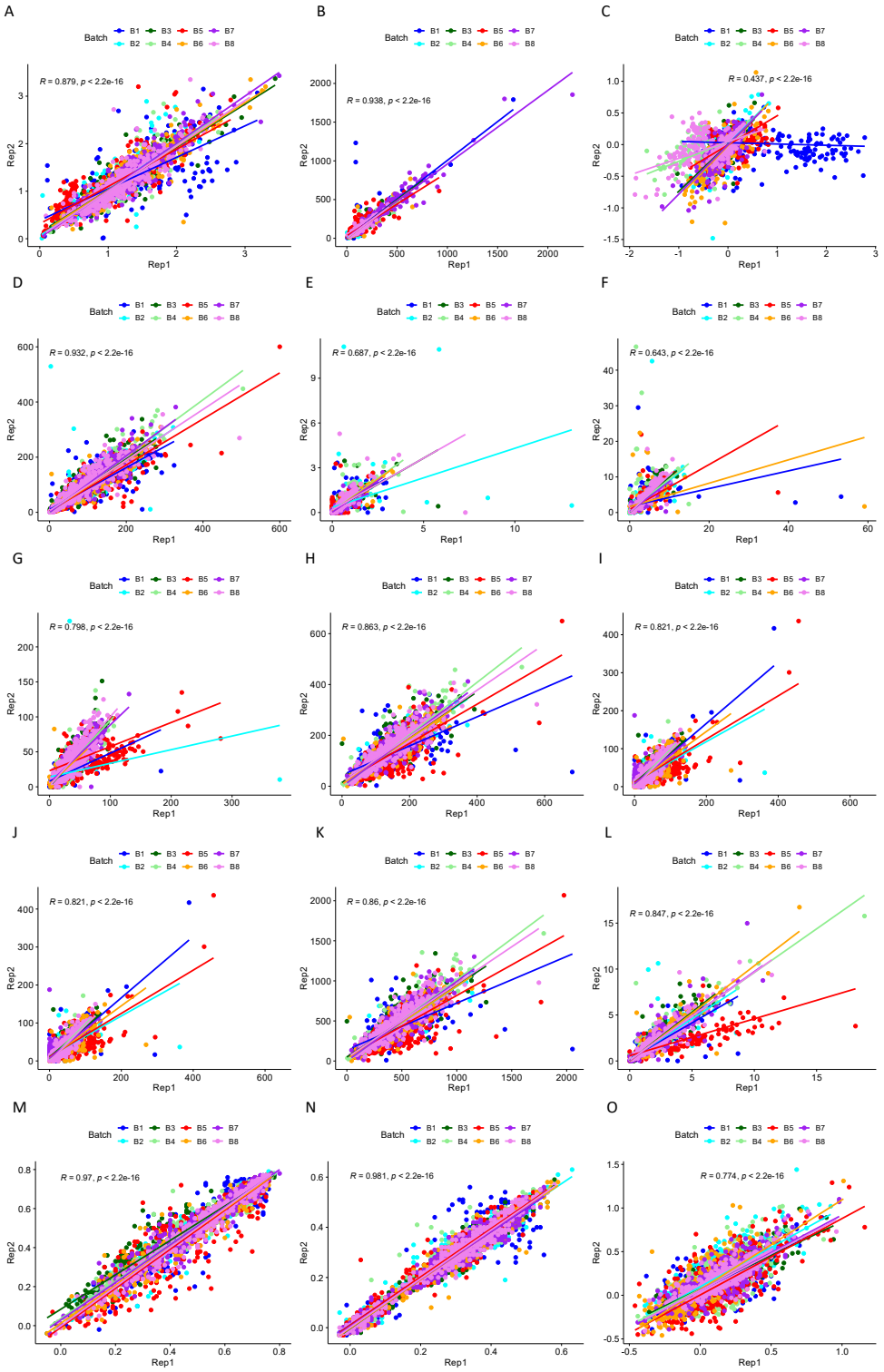

Figure S.III.12 Pearson correlation between the 2 replicates used to phenotype the MAGIC progeny, colour-coded by batch.
(A) Biomass, (B) OD fold-change, (C) Sedimentation, (D) [Ca], (E) [Cu], (F) [Fe], (G) [K], (H) [Mg], (I) [Mn], (J) [Na], (K) [P], (L) [Zn], (M) Fv/Fm, (N) ΦPSII, (O) NPQ

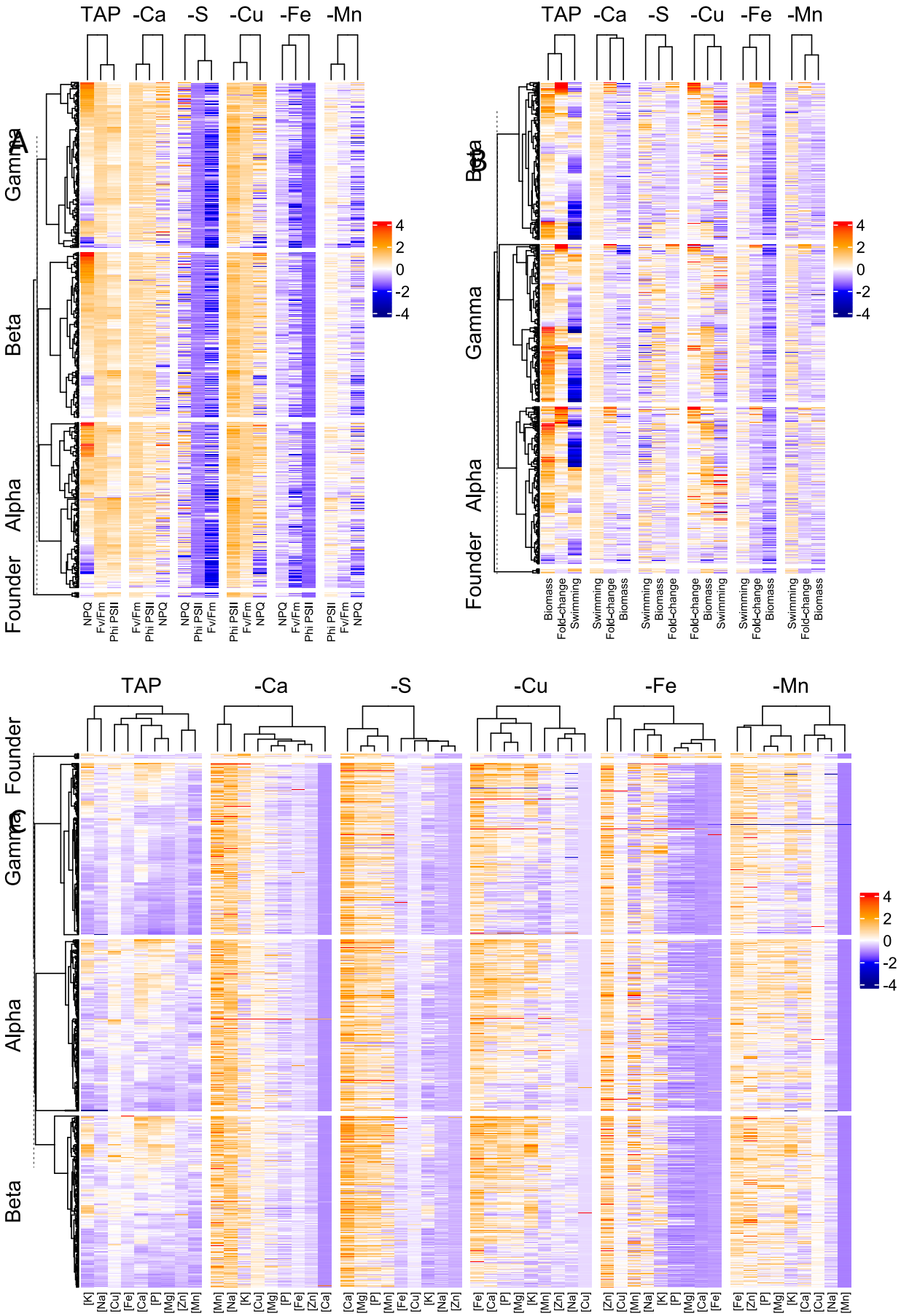

Figure S.III.13 Heatmap of the scaled phenotypic data, clustered by design. (A) Photosynthesis-related traits, (B) biomass-related traits, (C) ionome traits

A

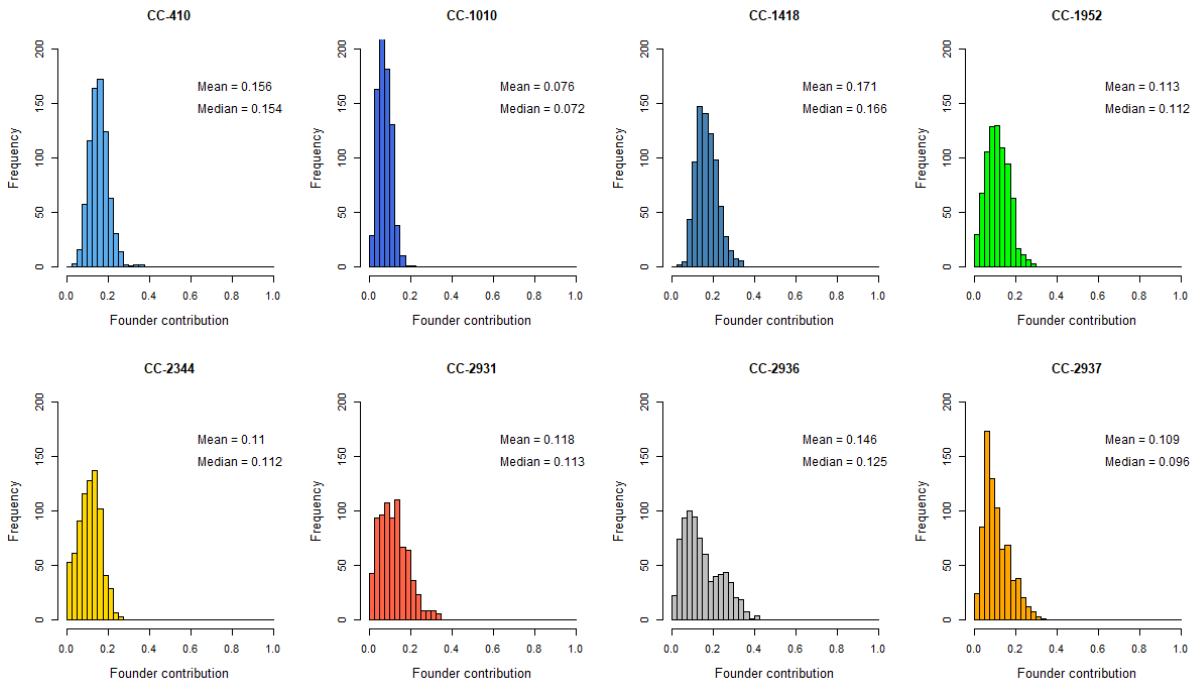

B

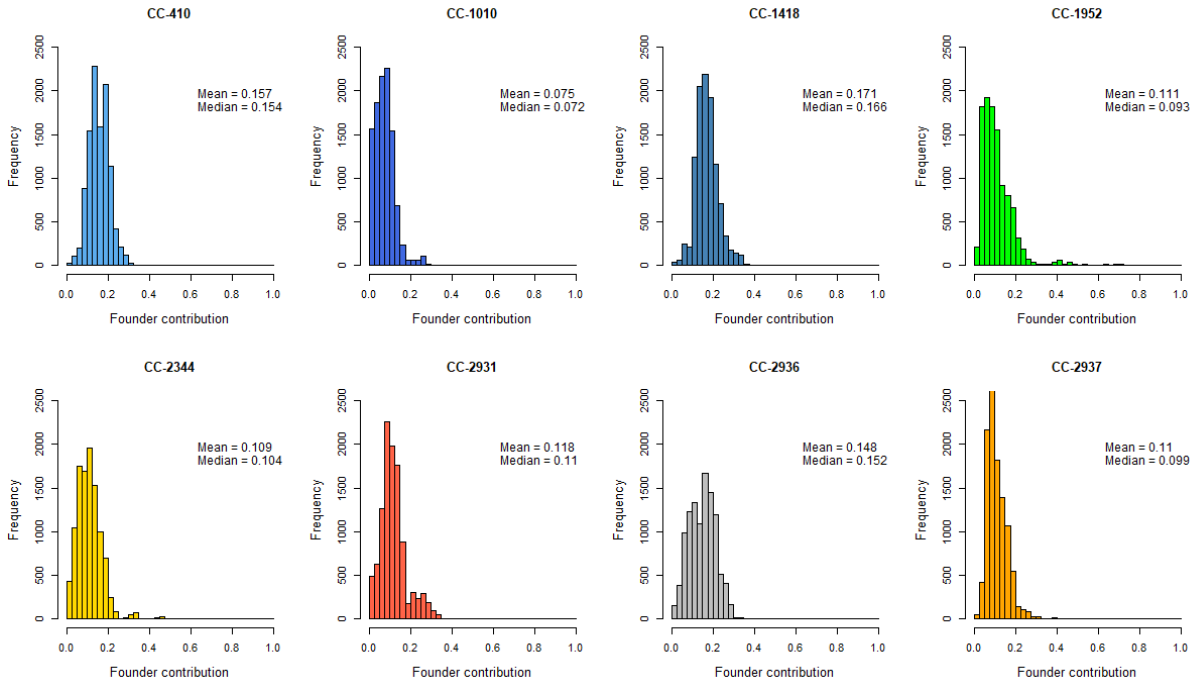

Figure S.III.14 Distribution of each founder's contribution (A) to each F8 line and (B) at each genomic position

Figure S.III.15 Genetic correlations within each of the 14 phenotypes measured in each of the 6 different media.
(A) Biomass, (B) OD fold-change, (C) Sedimentation, (D) Fv/Fm, (E) ΦPSII, (F) NPQ, (G) [Ca], (H) [Fe], (I) [K], (J) [Mg], (K) [Mn], (L) [Na], (M) [P], (N) [Zn]

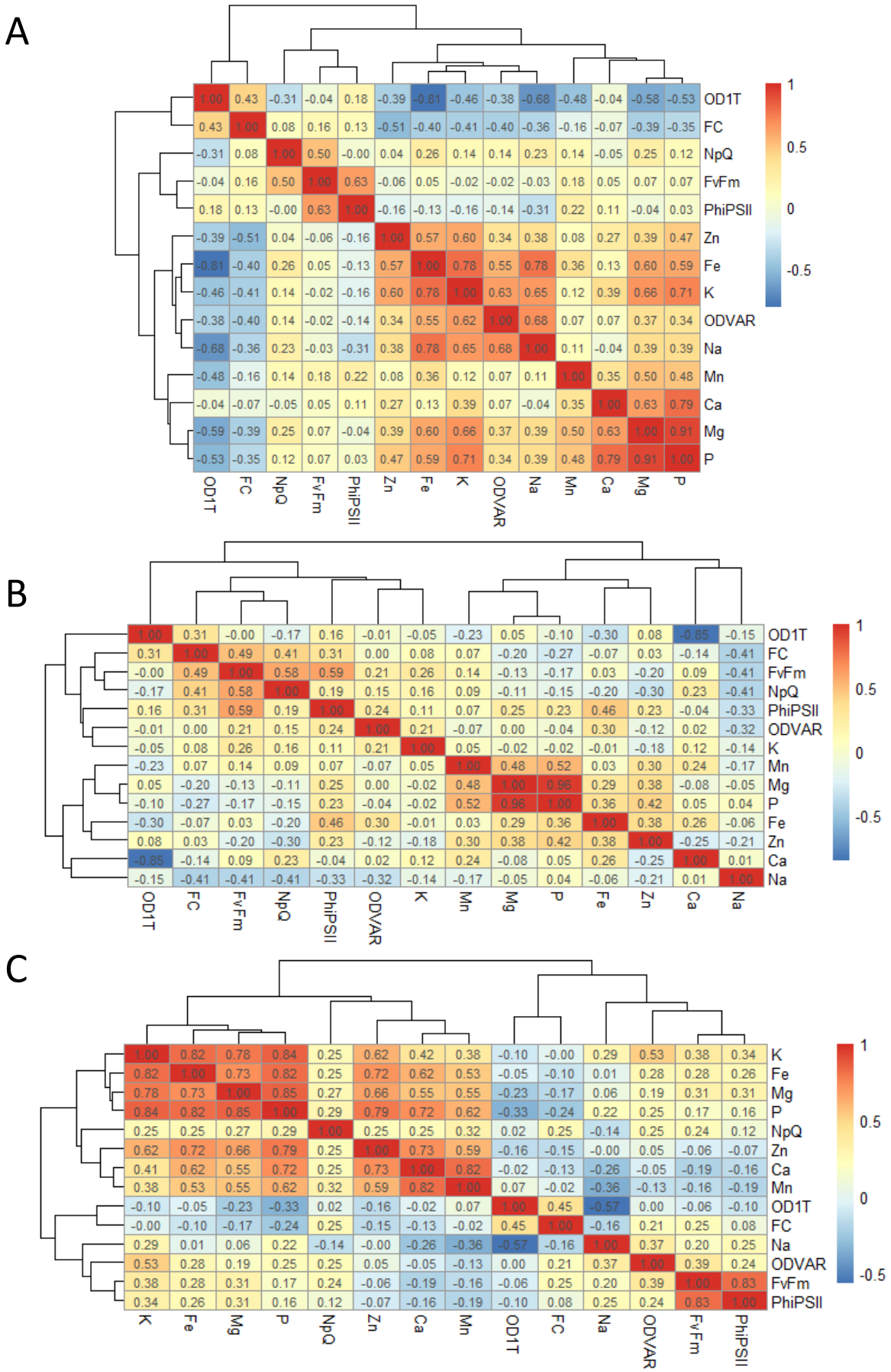

Figure S.III.16 Genetic correlations within each of the 6 media used to measure each of the 14 phenotypes. (A) TAP, (B) -Ca, (C) -S

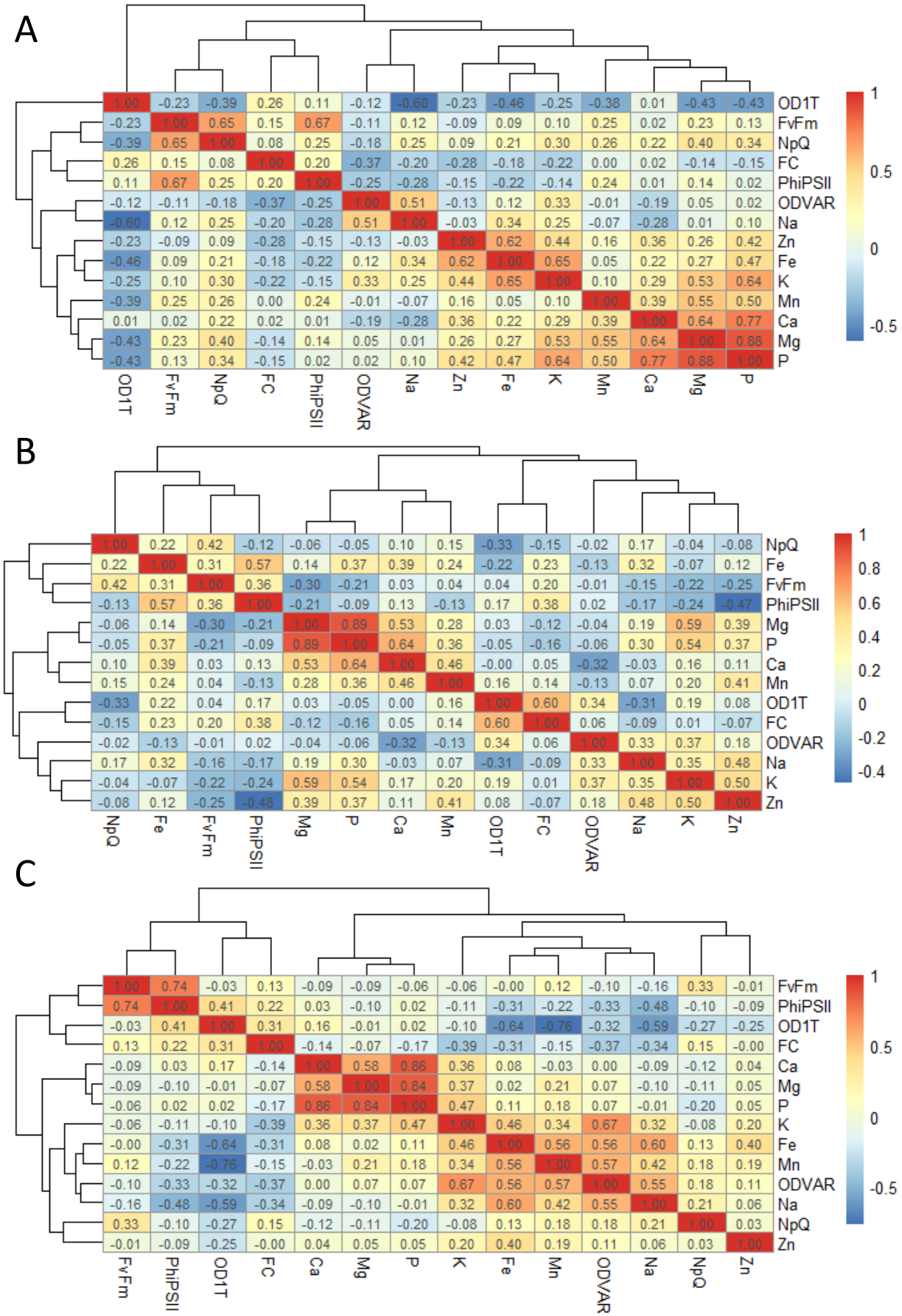

Figure S.III.17 Genetic correlations within each of the 6 media used to measure each of the 14 phenotypes (A) -Cu, (B) -Fe, (C)-Mn

Table S.III.1. Summary statistics of length of IBD segments shared between founder strains (length is expressed in kb).

Strain 1	Strain 2	Fraction IBD sites	Length		
			Median	Average	Max
CC-1952	CC-2931	0.097	0.70	1.42	63.91
CC-1952	CC-2344	0.072	0.82	1.94	181.33
CC-2344	CC-2931	0.103	0.93	2.03	174.99
CC-2937	CC-2344	0.035	1.32	2.77	104.38
CC-2936	CC-2344	0.031	1.54	3.15	118.42
CC-1952	CC-2937	0.023	1.22	3.17	85.81
CC-2936	CC-2931	0.023	1.40	3.20	132.86
CC-1952	CC-2936	0.021	1.54	3.27	104.03
CC-2937	CC-2931	0.030	1.24	3.40	281.80
CC-410	CC-1952	0.007	2.46	3.67	27.57
CC-1952	CC-1418	0.007	2.47	3.69	27.57
CC-410	CC-2931	0.007	2.17	4.04	31.19
CC-1418	CC-2931	0.007	2.17	4.04	31.19
CC-1010	CC-2344	0.019	2.25	4.30	139.75
CC-410	CC-2344	0.016	2.53	4.37	33.93
CC-1418	CC-2344	0.016	2.56	4.38	33.93
CC-1952	CC-1010	0.009	2.54	4.68	70.99
CC-1010	CC-2931	0.010	2.23	4.76	132.86
CC-1418	CC-2937	0.192	2.88	6.86	770.63
CC-410	CC-2937	0.191	2.88	6.86	770.63
CC-1010	CC-2937	0.202	2.70	6.89	770.63
CC-2936	CC-2937	0.236	2.30	7.05	831.59
CC-410	CC-2936	0.331	3.52	15.30	1067.92
CC-1418	CC-2936	0.331	3.52	15.30	1067.92
CC-1010	CC-2936	0.358	3.51	16.68	1790.81
CC-410	CC-1010	0.796	4.42	147.06	8596.03
CC-1010	CC-1418	0.796	4.42	147.06	8596.03
CC-410	CC-1418	1.000	6759.54	6552.93	9925.62